Nauplius
The Journal of The Brazilian Crustacean Society

e-ISSN 2358-2936
www.scielo.br/nau
www.crustacea.org.br

Original Article

Ontogenetic development captured in amber – the first record of aquatic representatives of Isopoda in Cretaceous amber from Myanmar

Mario Schädel[1] orcid.org/0000-0001-7945-4205
Matúš Hyžný[2] orcid.org/0000-0002-8960-2846
Joachim T. Haug[1,3] orcid.org/0000-0001-8254-8472

1 Ludwig-Maximilians-Universität München, Department of Biology II, Zoomorphology group. Großhaderner Straße 2, 82152 Planegg-Martinsried, Germany.

2 Comenius University in Bratislava, Department of Geology and Paleontology. Mlynská dolina, Ilkovičova 6, 842 15 Bratislava, Slovakia.

3 Ludwig-Maximilians-Universität München, GeoBio-Center. Richard-Wagner-Str. 10, 80333 München, Germany.

ZOOBANK: http://zoobank.org/urn:lsid:zoobank.org:pub:4817F86A-F0E9-41F8-B841-6B0A5ABE0221

Abstract

Two fossils from Burmese amber are the subject of this study. The specimens differ in size; yet, they appear to be conspecific because of the profound morphological similarity. The fossils are interpreted as representatives of Isopoda, more precisely of the group Cymothoida, due to the presence of a triangular basipod of the uropod. Cymothoida comprises parasitic forms of Isopoda as well as many other types of feeding-habits. The morphology in the studied fossils suggests that they are not representatives of any of the parasitic ingroups of Cymothoida. Since there are no other findings of Isopoda from the Cretaceous with the same morphological features, the fossils at hand are described as a new species – *Electrolana madelineae* sp. nov. The smaller specimen lacks well-developed walking appendages on trunk segment seven; it can thus be interpreted as a manca stage (immature) individual. The systematic affinity and the functional morphology of the herein described fossils, as well as three seed shrimps (Ostracoda) in close proximity to one of the specimens, and the presence of pyrite in the amber piece points towards an aquatic lifestyle and a preservation in moist conditions. In addition, we review the fossil record of immature forms of Isopoda.

Keywords

Juvenile, manca, ontogeny, pyrite, taphonomy

Corresponding Author
Mario Schädel
mario.schaedel@gmail.com

SUBMITTED 8 January 2020
ACCEPTED 8 September 2020
PUBLISHED 25 January 2021

DOI 10.1590/2358-2936e2021003

Introduction

General background

The majority of representatives of Isopoda are marine, with a high diversity of body shapes and fulfilling various ecological functions (Wägele, 1989; Brusca and Wilson, 1991; Brandt and Poore, 2003; Poore and Bruce, 2012). Oniscidea is the only lineage within Isopoda that successfully managed to establish a full terrestrial lifestyle, with more than 4,000 species (Brusca *et al.*, 2001; Schmalfuss, 2003).

The oldest fossil record of the group Isopoda in general reaches back into the Middle Pennsylvanian (Late Carboniferous, about 300 million years old) of Illinois (*Hesslerella shermani* Schram, 1970 from Mazon Creek). The Palaeozoic and most of the Mesozoic fossils of Isopoda are marine forms. Cretaceous amber from Myanmar (Cenomanian, about 99 million years old; Shi *et al.*, 2012) includes the oldest record of terrestrial representatives of Isopoda. However, the diversification of the terrestrial lifestyle must have occurred earlier, as the presence of several oniscidean lineages in Burmese amber suggests (Broly *et al.*, 2015; Poinar, 2018; Ross, 2019; Yu *et al.*, 2019).

Isopoda is an ingroup of Peracarida, hence its representatives share a special mode of brood care: the eggs develop in a brood pouch of the female, that is made-up of protrusions from the walking appendages (oostegites). This specialization is also preserved in the fossil record of Isopoda (Broly *et al.*, 2017) and other peracaridan lineages, including rather enigmatic extinct groups, such as Pygocephalomorpha (Pazinato *et al.*, 2016).

The extended brood care in Peracarida appears to be coupled with the loss of true larval stages during individual development (see discussion in Haug, 2020). In many lineages of Peracarida the offspring is thought to hatch from the egg as 'miniature versions of the adult' (Boyko and Wolff, 2014: 210); yet, this expression seems to be only a matter of detail, because, naturally, there are (small) differences between immatures and adults (Haug, 2019).

Within Peracarida one major lineage evolved a particular mode of post-embryonic ontogenetic development. Mancoidea is characterized by a specialized stage, a so-called manca stage, representing a strong autapomorphy of the group (Ax, 2000). Manca stage individuals lack fully developed appendages on the segment that holds the posterior-most walking appendages in the adult (Wägele, 1989; Ax, 2000; Boyko and Wolff, 2014) while already possessing fully functional appendages on the further posterior (pleon) segments. As Isopoda is an ingroup of Mancoida, manca stages are also found in representatives of Isopoda.

Within the group Cymothoida parasitic forms evolved. These parasitize fishes, crustaceans and occasionally other organisms (*e.g.* Cephalopoda; Hosie, 2008; Poore and Bruce, 2012). Parasites of crustaceans (Epicaridea) appear to have evolved from fish parasites (Dreyer and Wägele, 2001; Nagler *et al.*, 2017). Within Cymothoida, the parasitic feeding strategy likely evolved from a more generalist (hunting/scavenging) feeding type (Wägele, 1989; Nagler *et al.*, 2017). Within two of the parasitic lineages (Epicaridea and Gnathiidae) secondarily differentiated early post-embryonic stages evolved, that are generally considered to represent true larval stages (Boyko and Wolff, 2014) as they clearly fulfil numerous criteria such as: differing significantly from the adult in morphology and ecology; possessing structures that will be reduced later in ontogeny; being dispersal stages and also undergoing distinct metamorphosis (see Haug, 2020 for a longer discussion of the term 'larva' and its criteria).

Fossils of these parasitic lineages are quite rare, but often show characters that identify them as such and can give a clue about the systematic affinity of the fossils (Hansen and Hansen, 2010; Serrano-Sánchez *et al.*, 2015; Nagler *et al.*, 2017; Néraudeau *et al.*, 2017; Schädel *et al.*, 2019b). However, the systematic affinity of non-parasitic cymothoidans is often more problematic because many groups have only small-scaled apomorphic features that are unlikely to be accessible in fossils. Different approaches have been applied to solve the problem of systematic uncertainty by taxonomic practice. An overview of non-parasitic cymothoidans is given in Hyžný *et al.* (2013). Wieder and Feldmann (1992) tried to solve the problem by assigning new species to existing widespread groups with extant representatives – such as Cirolana. Jarzembowski *et al.* (2014) erected a new 'collective group' (= form-genus) for their non-parasitic cymothoidan fossil species.

Aside from these problems with the identification of fossil specimens, the main problem when dealing with new species is, that many ingroups of Cymothoida – such as Cirolanidae and many of its ingroups – cannot be characterized by apomorphic features and the monophyly of some of the groups is questionable (see discussion below).

Aims of this study

In this study we present the oldest currently known representatives of Cymothoida, which are preserved in amber. In most non-amber fossil sites, fossils of Isopoda are either strongly compressed or lack delicate structures such as the antennae. Thanks to the preservation in fossil resin, microscopic images, as well as micro-CT data, could be obtained. Based on two conspecific specimens we can show morphological differences that can be explained by ontogenetic development. The phylogenetic affinity is carefully discussed with respect to systematic problems within the group Cymothoida.

Geological settings

Burmese amber ('Burmite') refers to fossilized resin that is excavated in the Hukawng Valley in the northern part of Myanmar (Fig. 1A, map). Burmese amber has been dated to an age of *ca.* 99 million years (Cenomanian, Late Cretaceous) (Shi *et al.*, 2012). To prevent confusion with the younger, Late Cretaceous Tilin amber from central Myanmar (Zheng *et al.*, 2018), the amber from the Hukawng Valley is also termed Kachin amber. Palaeo-geographically, the Burmese amber site is located on the southern margin of the Eurasian Plate (Fig. 1B, map) and has a palaeolatitude of less than 22°N (Seton *et al.*, 2012; Mathews *et al*, 2016; Müller *et al.*, 2016; Scotese and Wright, 2018). The global temperature during the time of the amber deposition (early Cenomanian) is reconstructed to be relatively high and the decrease in temperature with increasing latitude was probably much lower than today (Voigt *et al.*, 2003; Price *et al.*, 2012); therefore a warm tropical climate can be assumed for the palaeoenvironment.

Material and Methods

Material

The two amber pieces in this study (Fig. S1A) have been commercially obtained by Mark Pankowski (Rockville, Maryland, USA), who kindly donated the pieces to the Natural History Museum Vienna (Naturhistorisches Museum Wien, NHMW), where the pieces are housed under the collection numbers 2017/0052/0001 and 2017/0052/0002. Further information on the geological background, except for the trade-name 'Burmese amber', is not available. The amber pieces likely stem from the mining areas near Noje Bum (Hukawng Valley, Kachin State, Myanmar), from where most of the commercially available Burmese amber pieces originate.

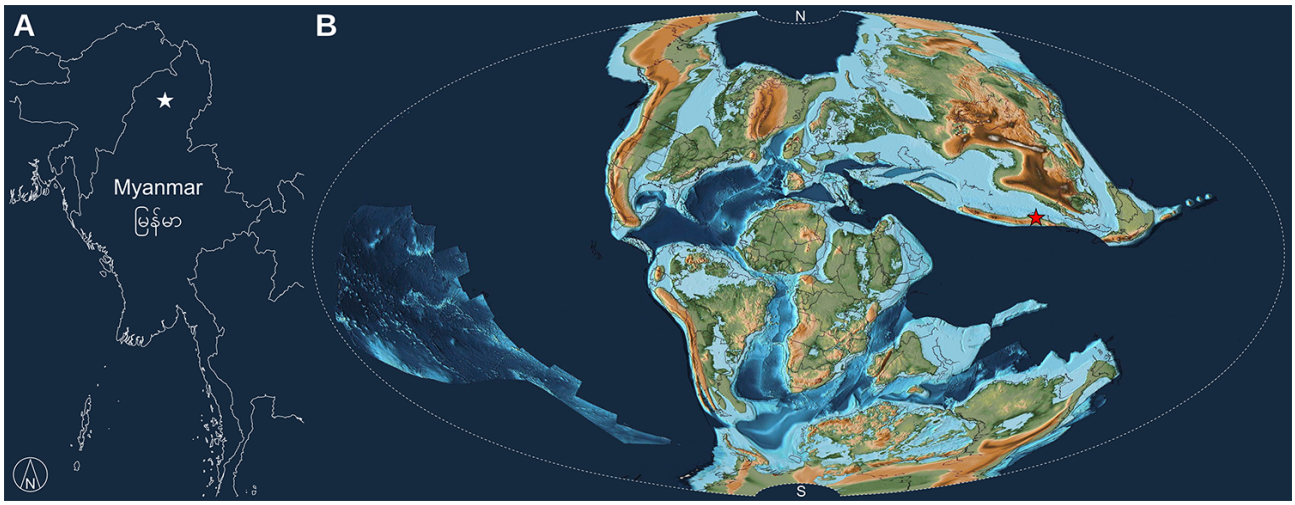

Figure 1. A: Map of Myanmar, white star marks the location of the Burmese amber mining sites near the town Noje Bum, base map from OpenStreetMap (openstreetmap.org); **B**: palaeogeographic world map, Aitov projection, 100 million years in the past, base image from PALEOMAP project (Scotese, 2016), red star marks the location of the Burmese amber sites.

Imaging

Microscopic images were gathered using a Keyence VHX-6000 digital microscope (VHX in the following). The implemented focus-merging function was used to overcome the limitations of the depth of field resulting from the high magnifications. Additionally, the implemented panoramic stitching function was applied in some cases to create high resolution images of larger objects. In-focus images from different view angles were gathered for further processing. In cases where the implemented focus-merging and panoramic stitching functions did not provide good results, stacks of images or individual in-focus images were recorded for further processing.

A Keyence BZ9000 digital fluorescence microscope (BZ in the following) was used to gather further microscopic images. Incident light with an excitation wavelength center of 545 nm (generally used for rhodamine-based stains, 'TRITC' filter cube) revealed the best contrast among the available fluorescence light sources (Haug *et al.*, 2011). Using the same microscope (BZ), transmitted-light microscopy was also performed. The native grey-value images gathered from the BZ9000 were saved for later processing.

For x-ray computer tomography (micro-CT) a Baker Hughes (General Electric) 'phoenix nanotom m' computer tomograph with a wolfram target on a cvd diamond was used along with the recommended acquisition software 'datos|x'. The scan was performed under a voltage of 100 kV. The amber piece was rotated 360 degrees in 1440 steps. The total scan time was 72 minutes. The final volume data was reconstructed using VGStudio MAX 2.2.6.80630 (Volume Graphics, proprietary). The achieved voxel size for the resulting stack of images (Fig. S5) was 2.81295 µm.

Processing

CombineZP (Alan Hadley, GPL) and Macrofusion (based on the Enfuse image blending algorithm, GPL) were used for combining stacks of images automatically to a single in-focus image (Mayer *et al.*, 2011). Drishti 2.6.4 was used for volume rendering of the micro-CT data (Hörnig *et al.*, 2016; Kypke and Solodovnikov, 2018). In one case, more than one transfer function was applied to show structures with different x-ray qualities. Two-dimensional images and red-cyan anaglyphs were exported from Drishti for further processing. GIMP 2.10 (GPL) was used to optimize the histogram, and enhance color, brightness and contrast of the final images. GIMP was also used to manually create panoramic images, background removal and to apply color markings to images (using layer masks, the colorize function and applying a shadow filter). Red-cyan stereo anaglyphs were created, using GIMP, to display three-dimensional structures (desaturation tool, colorize tool & layer transparency) (following Haug *et al.*, 2013).

QGIS 3.4.11 (GPL license) was used to assemble the maps. The map data for the map of Myanmar was obtained from OpenStreetMap (openstreetmap.org, ODbL license) via the QuickOSM plugin for QGIS. The palaeo-geographic map was retrieved from Scotese (2016) (PALEOMAP Project, www.earthbyte.org/paleomap-paleoatlas-for-gplates) and reprojected into Aitov projection (EPSG 53043) using QGIS. The palaeolatitude was calculated using the R package chronosphere (Kocsis and Raja 2020, GPL license) including multiple models (Seton *et al.*, 2012; Matthews *et al.*, 2016; Müller *et al.*, 2016; Scotese and Wright 2018). Inkscape (versions 0.92.3 and 0.92.4, GPL) was used to assemble the figure plates.

Use of generic names

Throughout the text, generic names are written in italics only when they are part of a binomial species name. This is a direct consequence of applying rank free nomenclature and, in addition, enhances the distinction between species names and names of higher systematic groups (with the exception of monospecific genera, all genus-ranked taxa are higher systematic groups and should represent monophyletic groups; *cf.* Schädel *et al.*, 2019b).

Results

Description of specimen NHMW 2017/0052/0002 (smaller specimen)

The body is composed of a distinct head (postocular segments 1–6, cephalothorax) and a trunk (postocular segments 7–19). The trunk is divided into two functional tagmata: the anterior trunk (pereon, postocular segments 7–13; posterior thorax) and the pleon (posterior trunk, postocular segments 14–19).

The last segment of the pleon is conjoined with the telson forming a pleotelson.

Body ovoid in dorsal view, tapering posteriorly, about 2.5 times longer than wide, widest at about half of the length. Dorsal surface with head capsule, tergites (robust dorsal sclerotization of the trunk segments) and pleotelson; surface largely with small rhomboid scales (Fig. 2A).

Head with anterior margin roughly semi-circular in dorsal view (Fig. 2A).

Eyes well developed, positioned laterally on the head, extending to the posterior margin of the head; ommatidia organised in an hexagonal array of at least 6 by 8 ommatidia (Fig. 2A–D).

Anteroventral side of the head with a complex formed by frontal lamina, clypeus and labrum. Anterior-most part (frontal lamina) with rhomboid anterior part, posterior part narrow with parallel lateral sides, prominent also in dorsal view; subsequent part (clypeus) connected to frontal lamina, but separated by a suture, triangular, shorter than wide, much wider than the posterior part of the frontal lamina; posterior-most part (labrum) connected to clypeus, but separated by a suture, about as wide as the posterior side of the clypeus (Fig. 3E).

Antennula (appendage of postocular segment 1) subdivided into a set of proximal peduncle elements and a set of distal flagellum elements; with at least two elongated peduncle elements and three or more, much shorter flagellum elements (distal elements not well visible) (Fig. 2A, B).

Antenna (appendage of postocular segment 2) subdivided into a set of proximal peduncle elements and a set of distal flagellum elements; three elongated peduncle elements and ten much shorter flagellum elements; proximal flagellum element about as wide as peduncle elements; flagellum elements continuously decreasing in width towards the distal most element; peduncle elements with setae on the distal margin, setae about one third of the length of the corresponding peduncle element (Fig. 2A, B).

Mandible (appendage of postocular segment 3) well developed, with proximal coxa and distal palp; mediodistal part ('pars incisivus', 'mandibular incisor') moderately broad; palp on the lateral side of the mandible ('mandibular palp'), well developed, composed of three or more elements; distal tip of mandibular palp with short setae (Fig. 3E).

Maxillula (appendage of postocular segment 4) narrow, distal tip with at least four setae (Fig. 3E).

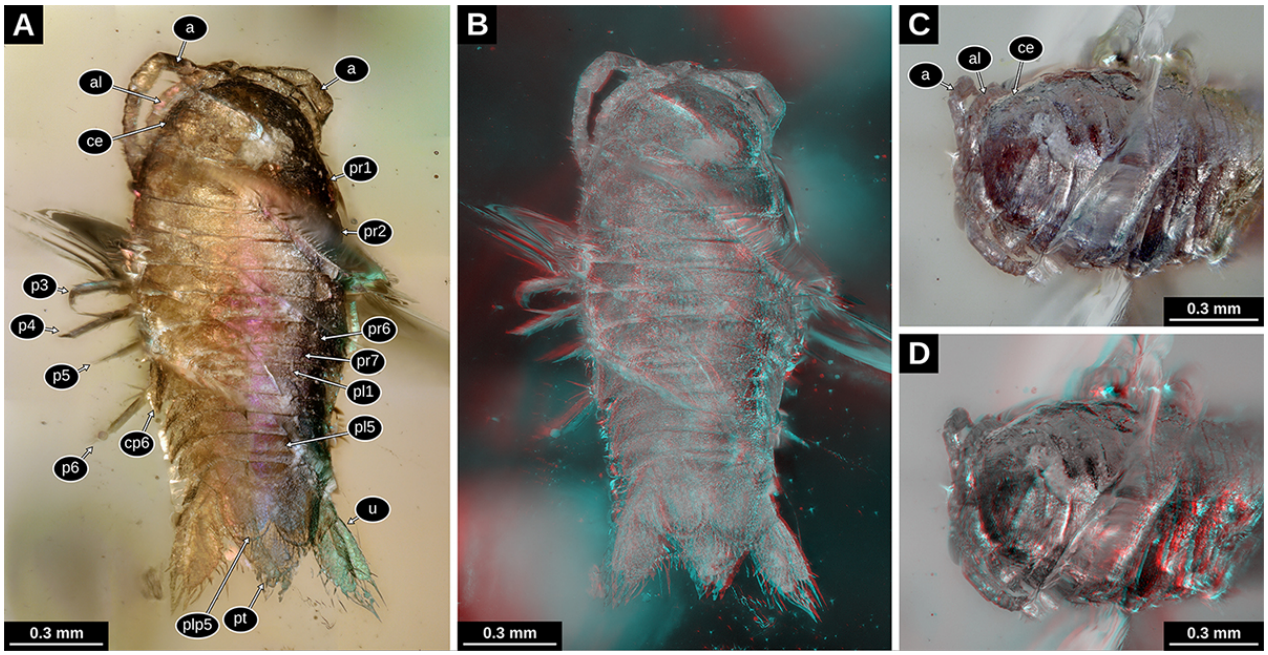

Figure 2. Paratype of *Electrolana madelineae* sp. nov. (NHMW 2017/0052/0002). **A**: Habitus in dorsal view, white light microscopy, coaxial light and polarising filter, 300x (VHX); **B**: habitus in dorsal view, red-cyan stereo anaglyph, white light microscopy, 200x (VHX); **C**: head region in antero-dorsal view, white light microscopy, 200x (VHX); **D**: head region in antero-dorsal view, red-cyan stereo anaglyph, white light microscopy, 200x (VHX). a, antenna; al, antennula; ce, compound eye; cp6, coxal plate of trunk segment 6; p3–6, trunk appendages 3–6; pl, pleon segments 1–5; plp5, pleopod 5; pr1–7, trunk segments 1–7; pt, pleotelson; u, uropod.

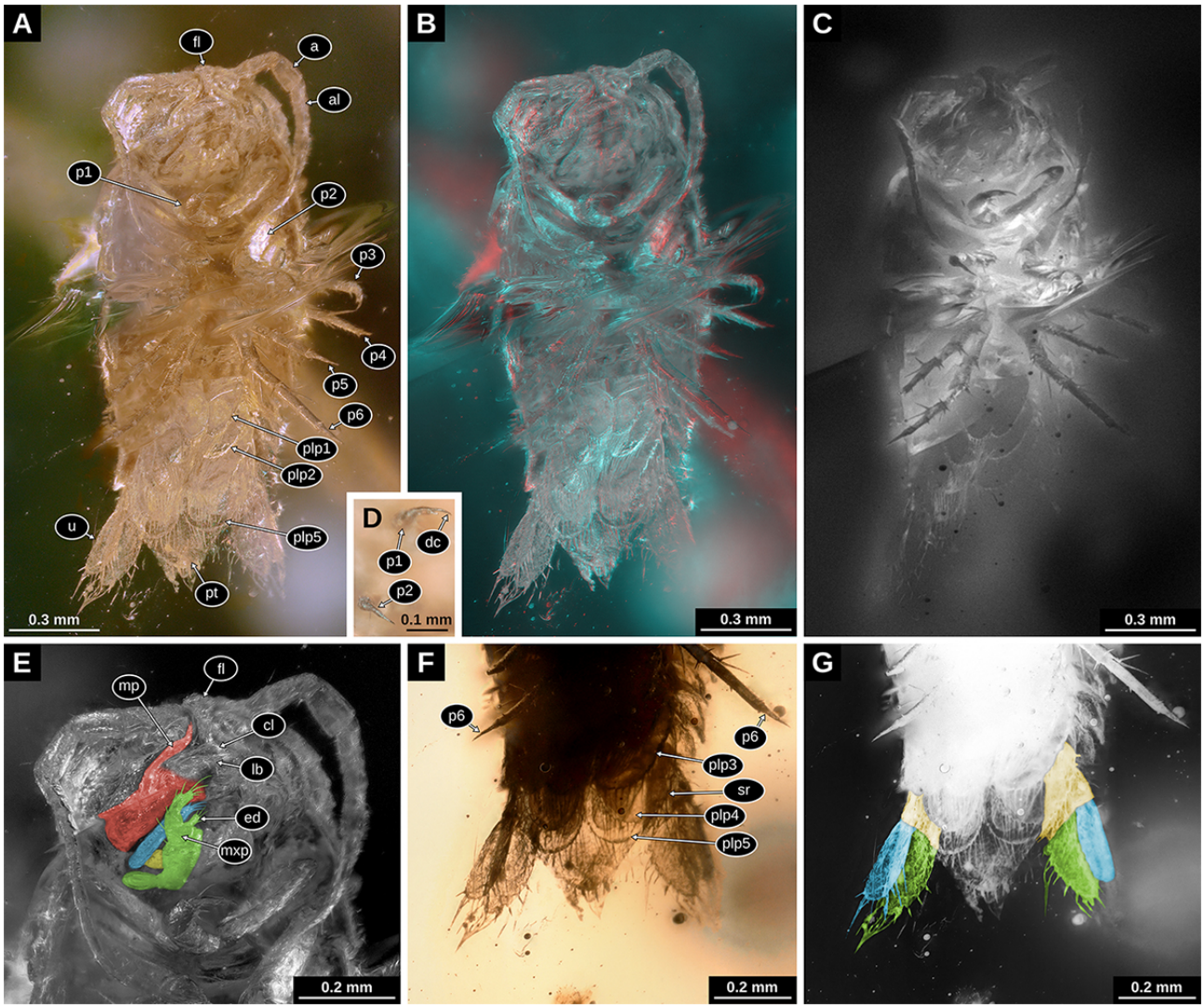

Figure 3. Paratype of *Electrolana madelineae* sp. nov. (NHMW 2017/0052/0002). **A**: Habitus in ventral view, white light microscopy, 300x (VHX); **B**: habitus in ventral view, red-cyan stereo anaglyph, white light microscopy, 200x; **C**: habitus in ventral view, epifluorescence microscopy, 4x (BZ); **D**: distal region of trunk appendages 1 and 2 in ventral view, right body side, white light microscopy, 300x (VHX); **E**: head in ventral view, white light microscopy, desaturated with colour markings, red mandible, blue maxillula, yellow maxilla, green maxilliped, 300x (VHX); **F**: pleon region in ventral view, white light microscopy, 300x (VHX); **G**: pleon region in ventral view, white light microscopy, desaturated and inverted, with color markings, yellow basipod, green endopod, blue exopod, 300x (VHX). a, antenna; al, antennula; cl, clypeus; dc, dorsal claw; ed, endite of the maxilliped; fl, frontal lamina; lb, labrum; mp, mandibular palp; mxp, maxilliped; p1–6, trunk appendages 1–6; plp1–5, pleopod 1–5; pt, pleotelson; sr, serration pattern; u, uropod.

Maxilla (appendage of postocular segment 5) present, but concealed by the appendage of the succeeding segment (Fig. 3E).

Maxilliped (appendage of postocular segment 6) composed of two proximal elements and a latero-distal palp (endopod?) inserting on the second element; proximal element elongated, originating on the postero-lateral side of the head and oriented medially along the ventral side of the head; distal element roughly rectangular, longer than broad; median margins of the distal elements of the left and right body side meeting each other along the medio-sagittal plane; distal element bearing an endite on the distal side and palp on the latero-distal side; endite narrow, with at least 4 prominent setae on the distal tip; palp composed of three elements; palp elements distally decreasing in width, each element with setae on the latero-distal corners; 4 prominent setae and multiple short setae on the distal tip of the palp (Fig. 3E).

Anterior trunk (pereon, postocular segments 7–13) dorsoventrally compressed, with 7 free tergites (tergites not conjoined with those of other segments).

Tergite of trunk segment 1 with concave anterior margin; longer along the lateral margins than along the midline; lateral margins gently convex (Fig. 2A, B).

Tergites of trunk segments 2–5 relatively uniform in shape, without concave anterior margins, shorter than the tergite of trunk segment 1 (Fig. 2A, B).

Tergite of trunk segment 6 about as long as the preceding tergites, with concave posterior margin (Fig. 2A, B).

Trunk segment 6 with a well-developed coxal plate (derivative of the proximal leg element); coxal plate triangular, with pointed postero-distal tip (Fig. 2A, B).

Tergite of trunk segment 7 (postocular segments 13) shorter than the preceding tergites, laterally encompassed by the tergite of trunk segment 6; without well-developed coxal plates (Fig. 2A, B).

Trunk segments 1–6 (postocular segments 7–12) with well-developed legs (thoracopods 2–7; pereopods 1–6); trunk segment 7 (postocular segment 13) without well-developed legs; trunk appendages 1–6 composed of 7 elements (coxa, basipod , and the five endopod elements: ischium, merus, carpus, propodus, dactylus); coxa not forming a distinct movable leg element, but forming scale-like extensions of the tergites (coxal plates) (Fig. 3A–C).

Distal part of trunk appendage 1 (distal to the coxa) with long basipod; ischium, merus and carpus much shorter than basipod; propodus moderately curved inward (median side concave), with setae on the median side and one long seta on the distal side; dactylus moderately curved inward, with two distinct tips ('claws') on the distal end, the more prominent one, in extension to the convex lateral side of the dactylus ('dorsal claw'; *cf.* Wägele, 1989; Wilson, 2009) distinct and much larger than the tip in extension to the concave median side of the dactylus ('ventral claw'; *cf.* Wägele, 1989; Wilson, 2009); dorsal claw with about the same level of curvature as the rest of the dactylus (Fig. 3A–D).

Distal part of trunk appendage 2 similar to trunk appendage 1; carpus triangular in anterior view; dorsal claw of dactylus distinct, but possible curvature not observable due to the viewing angle (Fig. 3A–D).

Distal part of trunk appendage 3 with small spines distally on the propodus; dactylus moderately curved; dorsal claw of the dactylus distinct and moderately curved (Fig. 3A–C).

Distal part of trunk appendage 4 with leg elements roughly cylindrical, all of them tapering distally; strong spines on the latero-distal side of the merus; propodus not curved; dactylus not curved (Fig. 3A–C).

Distal part of trunk appendage 5 with basipod long and antero-posteriorly compressed, distally increasing in width; ischium much shorter than basipod, antero-posteriorly compressed, distally increasing in width; merus antero-posteriorly compressed, about as long as ischium, more slender than ischium, with strong distal spines on the median side, with two strong and long spines on the lateral side; propodus roughly cylindrical, tapering distally; dactylus straight and conical, possible curvature only in the distal-most part (Fig. 3A–C).

Distal part of trunk appendage 6 with basipod long, antero-posteriorly compressed, distally increasing in width, with one strong distal spine on the median side and one strong distal spine on the lateral side; ischium similar to basipod, but of only about one third of the length of the basipod; merus not distally increasing in width, slightly antero-posteriorly compressed, two long and strong distal spines on the lateral side, strong but shorter distal spines on the median side; carpus and propodus sub-cylindrical, both with short distal spines on the median side; dactylus conical with pointed tip (Fig. 3A–C).

Posterior trunk, pleon (postocular segments 14–19) dorsoventrally compressed, with 5 free tergites.

Tergite of pleon segment 1 (postocular segment 14) short, laterally covered by the tergites of the preceding trunk segments 6 and 7 (Fig. 2A, B).

Tergite of pleon segment 2–4 (postocular segments 15–17) of about the same length and width, distinctly longer than the tergite of pleon segment 1 (postocular segment 14), lateral sides bent posteriorly and with pointed tips (Fig. 2A, B).

Tergite of pleon segment 5 (postocular segment 18) distinctly longer than the preceding segments, lateral margin with less distinct pointed tip (Fig. 2A, B).

Tergite of pleon segment 6 (postocular segment 19) conjoined with telson (pleotelson), triangular (angle between posterolateral margins about 75°), slightly

longer than wide, posterior tip rounded, posterior margin with 6 setae grouped around the posterior tip, serration pattern on the anterior part of the posterior margin (Figs. 2A, B, 3A, B, 3F, G).

Pleon segments 1–5 (postocular segments 14–18) with similarly shaped, flattened, appendages (pleopods), inserting on the ventral side of the body, composed of a proximal element (basipod) and two distal elements inserting on the basipod (endopod and exopod). Pleopods increasing in size from pleopod 1 to pleopod 5 (Fig. 3A–C, F, G).

Pleopod 1 basipod wider than long, with distal margin oblique, resulting median margin being much longer than lateral margin; endopod not visible, probably covered by the exopod; exopod longer than wide, median margin convex; distal margin rounded; distal margin with about 8 long setae (Fig. 3A–C).

Pleopod 2 basipod and endopod not visible; exopod similar to that of pleon segment 1, serration pattern at the distal margin (Fig. 3A–C).

Pleopod 3 basipod and endopod not visible; exopod similar to that of the preceding segments (Fig. 3A–C, F, G).

Pleopod 4 basipod not visible; exopod similar in shape to those of the preceding segments, with distinct serration pattern on the distal margin, setae inserting on the convex parts of the serration pattern; endopod narrower than the exopod, distal tip of endopod reaching more distally than the tip of the exopod (Fig. 3A–C, F, G).

Pleopod 5 basipod not visible; endopod more slender than exopod, no setae on distal margin; exopod with rounded distal margin, distal margin with long setae, serration pattern of the distal margin weaker than that in the exopod of pleopod 4 (Fig. 3A–C, F, G).

Pleon segment 6 (postocular segment 19) with appendages inserting on the ventrolateral side of the body (uropods). Basipod roughly triangular in shape, lateral margins without visible setae; endopod elongated, longer than wide, about 2.5 times, distal margin rounded, strong and long setae on the distal margin and the distal part of the median margin; exopod elongated, more slender than the endopod, longer than wide, about 3 times, distal margin rounded, some weak setae on the lateral margins, strong and long setae on the distal margin and the distal part of the median margin (Fig. 3A–C, F, G).

Measurements of specimen NHMW 2017/0052/0002 (smaller specimen)

Body length (without appendages) 1.72 mm; maximal body width (without appendages) 0.70 mm; head length 0.35 mm; head width 0.51 mm; antenna length (two-dimensional measurement) 0.71 mm (left), 0.85 mm (right); anterior trunk length 0.64 mm; trunk tergite 1 length 0.14 mm; trunk tergite 2 length 0.09 mm; trunk tergite 3 length 0.10 mm; trunk tergite 4 length 0.09 mm; trunk tergite 5 length 0.08 mm; trunk tergite 6 length 0.08 mm; trunk tergite 7 length 0.06; pleon length without pleotelson 0.33 mm; pleon segment 1 length 0.04 mm; pleon tergite 2 length 0.06 mm; pleon tergite 3 length 0.07 mm; pleon tergite 4 length 0.07 mm; pleon tergite 5 length 0.09 mm; pleotelson length 0.39 mm.

Syn-inclusions of specimen NHMW 2017/0052/0002 (smaller specimen)

Isolated leg, Euarthropoda (Fig. S2A); isolated distal element of a leg, Euarthropoda (Fig. S2B); mite (Arachnida: Acari) (Fig. S2C–E); possible cuticle remains, Euarthropoda (Fig. S2F); multiple needle-like objects, possibly plant hairs or setae of euarthropodans (Fig. S2G).

Description of specimen NHMW 2017/0052/0001 (larger specimen)

Body organization, see description above. Body drop shaped (dorsal view), tapering posteriorly, about 2.2 times longer than wide, widest at about half of the length (Figs. 4A, 5A–C, 6). Dorsal surface with head capsule, tergites (robust dorsal sclerotizations of the trunk segments) and the pleotelson.

Head with anterior margin roughly half-circular in dorsal view (Fig. 5A).

Eyes well developed, positioned laterally on the head (Fig. 4E). Anterior margin of the head without distinct median process (rostrum), separated from the frontal lamina (Fig. S1D).

Antennula (appendage of postocular segment 1) subdivided into a set of proximal peduncle elements and a set of distal flagellum elements; with three elongated peduncle elements and nine or more, much shorter, flagellum elements (Figs. 4B,C, E, 5A).

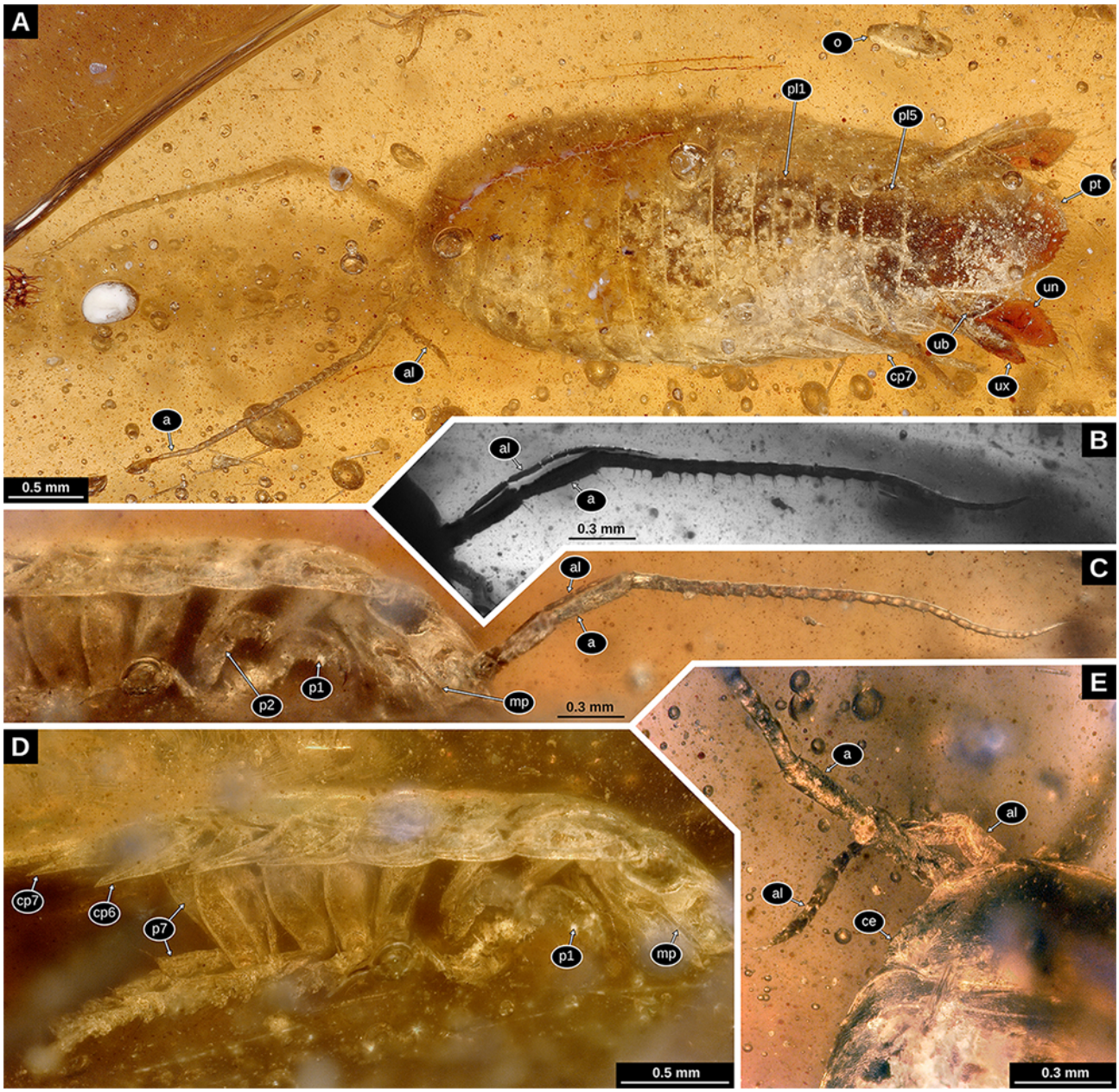

Figure 4. Holotype of *Electrolana madelineae* sp. nov. (NHMW 2017/0052/0001). **A**: Habitus in dorsal view, white light microscopy, 200x (VHX). **B**: anterior head region in ventro-lateral view, transmitted light microscopy, 4x (BZ); **C**: anterior body region in ventro-lateral view, white light microscopy, 200x (VHX); **D**: anterior trunk region in ventro-lateral view, white light microscopy, 150x (VHX); **E**: head region in dorsal view, left body side, white light microscopy, 200x (VHX). a, antenna; al, antennula; ce, compound eye; cp6–7, coxal plate of trunk segment 6–7;mp, mandibular palp; o, seed shrimp (Ostracoda); p1–7, trunk appendages 1–7; pt, pleotelson; ub, uropod basipod; un, uropod endopod; ux, uropod exopod.

Antenna (appendage of postocular segment 2) subdivided into a set of proximal peduncle elements and a set of distal flagellum elements; three elongated peduncle elements and twenty-two much shorter flagellum elements; proximal peduncle element about two times longer than wide; second and third peduncle element of about the same shape and size, much longer than the proximal peduncle element, a set of two setae on the ventral side of the distal end of the elements; proximal flagellum element distinctly narrower than the peduncle elements; flagellum elements continuously decreasing in width towards the distal most element, a set of two setae on the ventral side of the distal end of the elements; long seta on the distal end of the distal most flagellum element (Figs. 4A–C, 5A–D).

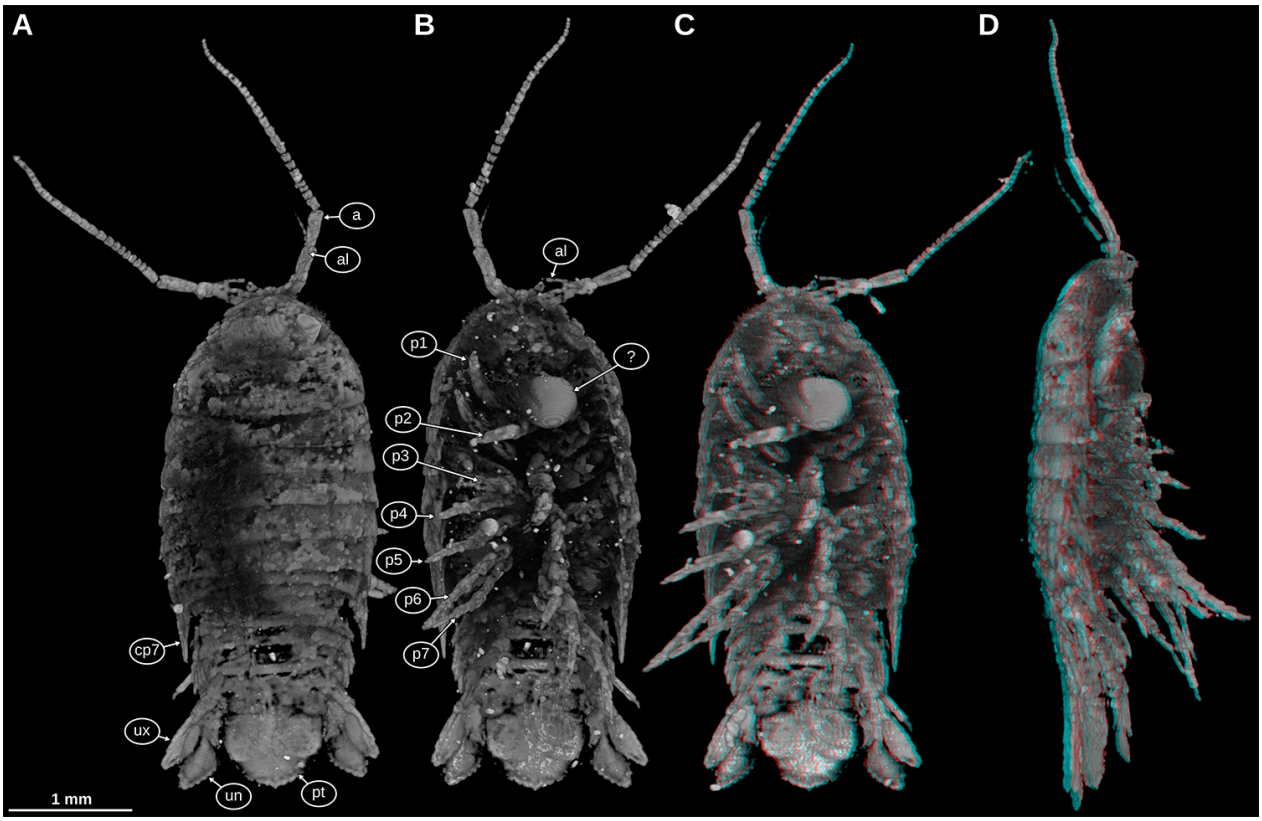

Figure 5: Holotype of *Electrolana madelineae* sp. nov. (NHMW 2017/0052/0001), volume rendering images based on micro-CT data. **A**: Habitus in dorsal view, orthographic projection; **B**: habitus in ventral view, orthographic projection; **C**: habitus in ventral view, red-cyan stereo anaglyph, perspective projection; **D**: habitus in lateral view, right body side, red-cyan stereo anaglyph, perspective projection. a, antenna; al, antennula; cp7, coxal plate of trunk segment 7; p1–6, trunk appendages 1–6; pt, pleotelson; un, uropod endopod; ux, uropod exopod; ?, unknown material forming an irregular bubble.

Mandible (appendage of postocular segment 3) well developed, with coxa and distal palp; mandibular palp well developed, composed of a wide proximal element and one or more much narrower distal elements, distal elements together about three times longer than proximal element (Fig. 4C).

Anterior trunk (pereon, postocular segments 7–13) dorsoventrally compressed, with 7 free tergites (tergites not conjoined with those of other segments).

Tergite of trunk segment 1 (postocular segment 7) with concave anterior margin; longer along the lateral margins than along the midline; lateral margins convex (Figs. 4A, 5A).

Tergites of trunk segments 2–5 (postocular segments 8–11) relatively uniform in shape, without concave anterior margins, shorter than the tergite of trunk segment 1 (Figs. 4A, 5A).

Tergite of trunk segment 6 (postocular segment 12) about as long as the preceding tergites, with gently concave posterior margin (Fig. 4A).

Tergite of trunk segment 7 (postocular segment 13) much shorter along the midline than the preceding tergites, laterally not encompassed by the tergite of trunk segment 6 (Fig. 4A).

Trunk segment 1 (postocular segment 7) seemingly without coxal plate (derivative of the proximal leg element, laterally adjoining the tergite); trunk segment 2 and 3 with sub-rectangular coxal plates, ridge on the dorsal side of the plate curved, distally approaching the lateral margin; trunk segment 4–7 (postocular segments 10–13) with well-developed triangular coxal plates, plates triangular, with pointed postero-distal tip, increasing in size towards trunk segment 7 (postocular segment 13); coxal plates 6 and 7 (postocular segment 12-13) with oblique straight ridge on the dorsal side of the plate, distally joining the postero-distal corner; coxal plate of trunk segment 7 very conspicuous in dorsal view, extending distally to the level of pleon segment 5 (postocular segment 18) (Figs. 4A, D, 5A–D).

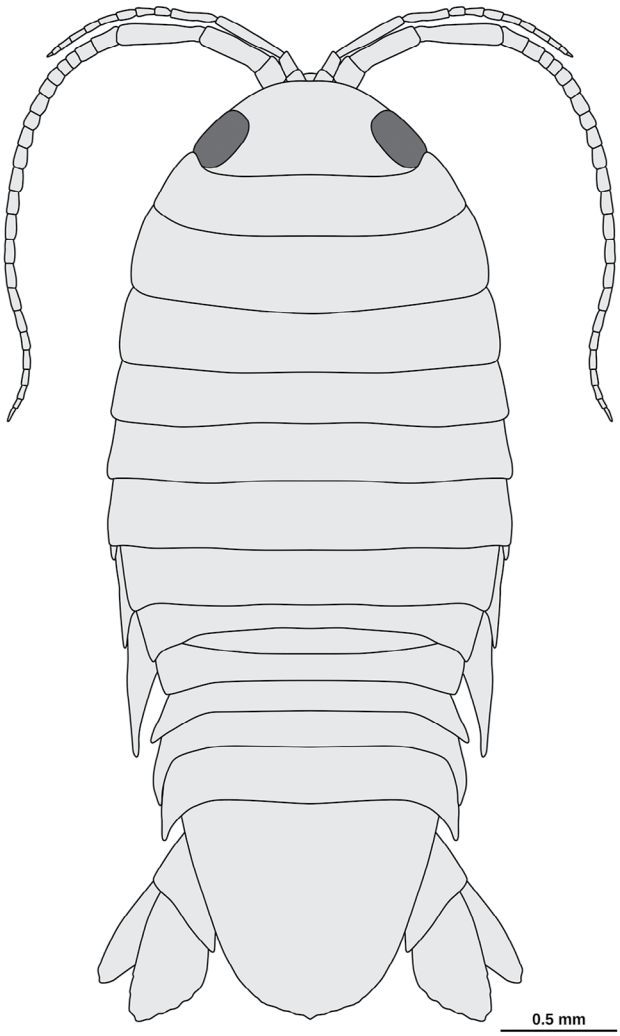

Figure 6. Drawing of the holotype of *Electrolana madelineae* sp. nov. (NHMW 2017/0052/0001), dorsal view, composite of microscopic images and micro-CT scan data.

Trunk segments 1–7 (postocular segment 7–13) with well-developed legs (thoracopods 2–7, pereopods 1–6); trunk appendages composed of 7 elements (coxa, basipod, and the five endopod elements: ischium, merus, carpus, propodus, dactylus); coxa not forming a distinct movable leg element but forming scale-like extensions of the tergites (coxal plates) (Figs. 4C, D, 5B–D).

Distal part of trunk appendage 1 (distal to the coxa; postocular segment 7) with long basipod; ischium, merus and carpus much shorter than basipod; propodus slightly curved inward (median side concave), with setae on the median side; dactylus much shorter and narrower than the propodus, curved inward, with a distinct claw, claw curved inward and much darker than the rest of the dactylus (Figs. 4C, 5B–D and volume data).

Distal part of trunk appendage 2 similar to trunk appendage 1; ischium much shorter than basipod; merus and carpus shorter than ischium, carpus triangular in posterior view (Figs. 4C, 5B–D and volume data).

Distal part of trunk appendage 3 roughly similar to the two preceding trunk appendages; propodus slightly curved inward (Fig. 5C and volume data).

Distal part of trunk appendage 4 longer than trunk appendage 3; carpus distally increasing in width; propodus straight and roughly cylindrical; dactylus short and straight (Fig. 5C and volume data).

Distal part of trunk appendage 5 (postocular segment 11) longer than trunk appendage 4; basipod broad, with posterior margin convex, median ridge along the midline of the lateral surface; ischium almost as long as basipod; merus and carpus of about half of the ischium, each distally increasing in width and slightly compressed in antero-posterior direction; propodus slightly compressed in antero-posterior direction, median margin slightly concave; dactylus short and pointed, very weakly curved inward (Figs. 4D, 5C, D and volume data).

Distal part of trunk appendage 6 (postocular segment 12) longer than trunk appendage 5 (longest trunk appendage); basipod broad, with posterior margin convex, median ridge along the midline of the lateral surface; ischium long and slender, distally increasing in width and more antero-posteriorly compressed; merus and carpus of similar shape, both antero-posteriorly compressed, distally increasing in width; propodus slightly compressed in antero-posterior direction, median margin slightly concave; dactylus short and pointed, very weakly curved inward (Figs. 4D, 5C, D and volume data).

Distal part of trunk appendage 7 similar to trunk appendage 6, but distinctly shorter; ischium with long seta distally on the lateral side; merus with seta distally on the lateral side (Fig. 5C, D and volume data).

Posterior trunk, pleon (postocular segments 14–19) dorsoventrally compressed, with 5 free tergites.

Tergite of pleon segment 1 short, laterally covered by the tergites of the preceding trunk segment 7 (Figs. 4A, 5A, 7A).

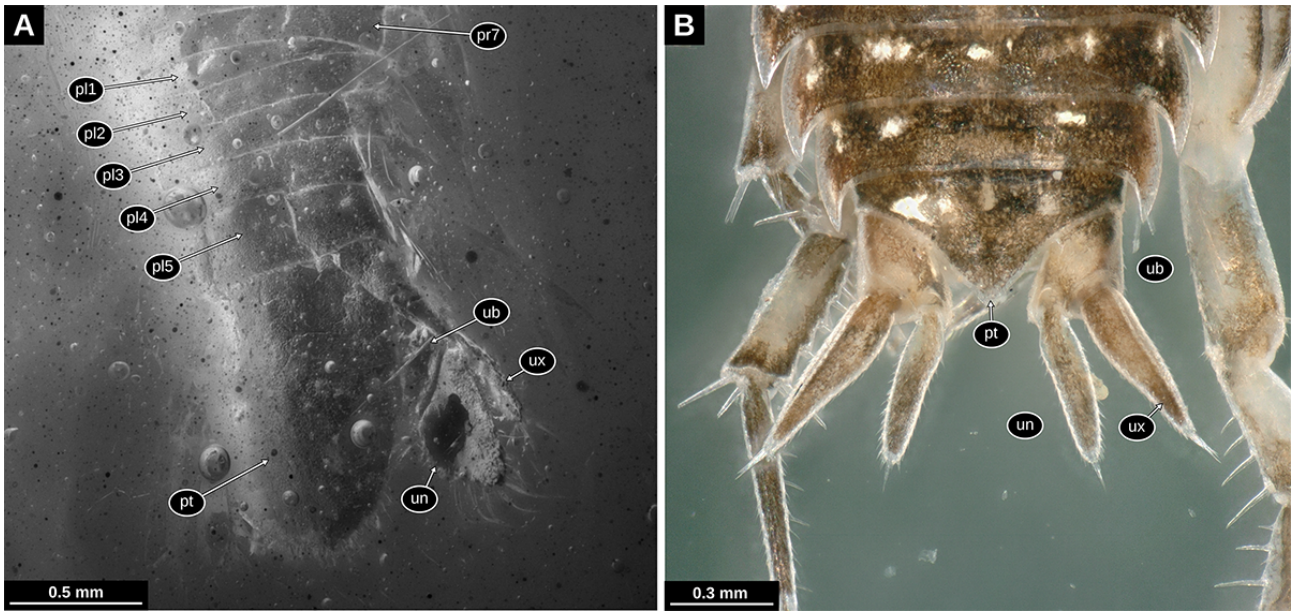

Figure 7. Comparison of the uropod morphology between *Electrolana madelineae* sp. nov. and an extant representative of Oniscidea. **A**: Holotype of *Electrolana madelineae* sp. nov. (NHMW 2017/0052/0001), pleon region in latero-dorsal view, epifluorescence microscopy, 4x (BZ); **B**: *Philoscia* cf. *muscorum* (Scopoli, 1763), posterior pleon region in dorsal view, white light microscopy, 200x (VHX). pl, pleon segments 1–5; pr7, trunk segment 7; pt, pleotelson; ub, uropod basipod; un, uropod endopod; ux, uropod exopod.

Tergites of pleon segments 2–4 (postocular segments 15–17) of about the same length and width, slightly longer than the tergite of pleon segment 1, lateral sides bent posteriorly and with pointed tips (Figs. 4A, 5A, 7A).

Tergite of pleon segment 5 (postocular segment 18) distinctly longer than the preceding segments (Figs. 4A, 5A, 7A).

Tergite of pleon segment 6 (postocular segment 19) conjoined with the telson (pleotelson) half-oval, slightly longer than wide; anterior margin straight; posterior tip rounded with median notch/tooth, posterior margin with numerous setae grouped in the posterior-most part (Figs. 4A, 7A).

Pleon segments 1–4 (postocular segments 14–17) with appendages not visible (not preserved, not visible and without x-ray contrast). Appendage of pleon segment 5 (pleopod 5; postocular segment 18) with only exopod visible, exopod broad, flattened and with rounded posterior margin, numerous long setae on the distal margin (Fig. 5B, C).

Pleon segment 6 (postocular segment 19) with appendages roughly similar to those of the preceding segments but inserting on the ventrolateral side of the body (uropods). Uropod basipod roughly triangular in shape, lateral margins without visible setae; endopod elongated, about 2 times longer than wide, median margin with weak angle, fine setae on the lateral margin, strong and long setae on the distal margin and the distal part of the median margin; exopod elongated, more slender than the endopod, about 3 times longer than wide, distal margin with an acute angle, strong and long setae on the distal margin and the distal part of the median margin (Figs. 4A, 5B, C, 7A).

Measurements of specimen NHMW 2017/0052/0001 (larger specimen)

Body length (without appendages) 4.00 mm; maximal body width (without appendages) 1.79 mm; head length 0.58 mm; head width 1.01 mm; antennula length (two-dimensional measurement) 0.95 mm (left), 0.81 mm (right); antenna length (two-dimensional measurement) 2.38 mm, peduncle length 0.76 mm, flagellum length 1.62 mm (left), 2.62 mm, peduncle length 0.85 mm, flagellum length 1.77 mm (right); anterior trunk length 1.93 mm; trunk tergite 1 length 0.57 mm; trunk tergite 2 length 0.25 mm; trunk tergite 3 length 0.22 mm; trunk tergite 4 length 0.26 mm; trunk tergite 5 length 0.29 mm; trunk tergite 6 length 0.25 mm; trunk tergite 7 length 0.12;

pleon length without pleotelson 0.72 mm; pleon segment 1 length 0.12 mm; pleon tergite 2 length 0.13 mm; pleon tergite 3 length 0.14 mm; pleon tergite 4 length 0.15 mm; pleon tergite 5 length 0.26 mm; pleotelson length 0.93 mm.

Syn-inclusions of specimen NHMW 2017/0052/0001 (larger specimen)

Fly, Diptera *cf.* Psychodidae (Fig. S3A, B); Alavesia (Fig. S3C, D); beetle, Coleoptera (Fig. S3E, F); remains, Euarthropoda (Fig. S4A); two isolated but closely grouped legs, Euarthropoda (Fig. S4B–C); isolated leg, Euarthropoda (Fig. S4D); three individuals of seed shrimps, Ostracoda (Fig. S4E–G).

Discussion

Conspecificity of the two specimens and ontogenetic changes

Except for the body size, the two herein studied specimens are overall very similar.

Nevertheless, there are morphological differences between the two studied fossil specimens: 1) The antennae are proportionally longer, more slender and consist of a larger number of flagellum elements in the larger specimen (Fig. 3A *vs.* Fig. 4C). 2) The trunk appendage 7 is only well developed in the larger specimen (Fig. 3A–C *vs.* Fig. 4D). 3) The posterior margin of the pleotelson is more rounded and less triangular in shape in the larger specimen (Fig. 2A *vs.* Fig. 5A). 4) The distal ends of the uropods are more acute and less rounded in the larger specimen (Fig. 3F *vs.* Fig. 4A). Considering the similarity between the two specimens and that the differences can easily be explained by ontogenetic changes, it appears most likely that the two specimens are conspecific.

Most representatives of Isopoda develop at first in a specialised brood pouch of the female (Boyko and Wolff, 2014). Early post-embryonic stages lack a well-developed seventh trunk appendage (manca stage; Ax, 2000; Boyko and Wolff, 2014). The seventh pair of trunk appendages develops well after the immature offspring escapes from the brood pouch; the development of these appendages marks the end of the manca stage (Boyko and Wolff, 2014). The smaller specimen (NHMW 2017/0052/0002) can clearly be interpreted as a manca stage, due to the absence of a well-developed seventh trunk appendage.

The transition between the manca stage and the (following) juvenile or adult stage in the herein described Cretaceous species must have occurred while the individuals were 1.72 to 4 mm long. This of course cannot be generalized for the entire population, as there can be considerable variation in the sizes of individuals (*cf.* size ranges of manca stages in Bruce, 1986; Brusca *et al.*, 1995). Only in the group Bathynomus manca stage individuals are much larger (up to 60 mm body length) – likely due to the enormous size of the adults (Soong and Mok, 1994).

After 'Dyar's law' (Dyar, 1890) or 'Brook's law' (Fowler, 1904) the growth in representatives of Euarthropoda measured in areas of the bodies that are not affected by inter-moult growth, follows a constant coefficient ('*r*' in the following). The application of Dyar's law/Brook's law certainly has its limitations, since with some exception, *e.g.*, (most) flying insects, the number of moults in the life of individuals is not limited ('life-long growth'). A decrease of the growth coefficient *r* with increasing size and age, especially after reaching maturity, has to be expected. Nevertheless, in early stages of the development of non-insectan crustaceans, such as those of the group Isopoda, a more or less linear growth with each moult can be expected (Minelli and Fusco, 2013).

Assuming a linear growth, the growth coefficient *r* can be calculated with the following formula, when a certain length before (X_{i-n}) and after (X_i) the moult or multiple (n) moulting events are known.

$$r = (X_i / X_{i-n})^{1/n}$$

Growth coefficients of 1.2 to 1.44 have been shown for extant aquatic forms of Isopoda, that have not yet reached sexual maturity (Strong and Daborn, 1979; Luxmoore, 1981; Johansen, 2000). Assuming that both fossils are neither especially small nor large for their respective ontogenetic stage, the most likely assumption is that there are two or three intermediate instars (three or four moults) between them (Tab. 1).

Table 1. Growth coefficients calculated for *Electrolana madelineae* sp. nov. for different numbers of moults assumed to have happened between the preserved stages, calculated based on the overall-body length of the holotype and the paratype.

n (Number of potential moulting events)	Growth coefficient
1	2.33
2	1.52
3	1.32
4	1.23
5	1.18

Systematic interpretation of the herein described fossils

With the presence of a manca stage juvenile, the herein studied species can be considered as a representative of Mancoidea (including Cumacea, Mictacea, Spelaeogriphacea, Tanaidacea and Isopoda; Ax, 2000). Though there are no apomorphic features for Isopoda visible in the fossils, the overall morphology only matches Isopoda and not any of the other mancoideans ingroups. Specialised proximal elements of the trunk appendages 2–7 (coxal plates) are an autapomorphy of the group Scutocoxifera (Dreyer and Wägele, 2002), which is an ingroup of Isopoda. The triangular shaped basipod of the uropods (Fig. 3F, G) is an autapomorphy of Cymothoida (a large ingroup of Scutocoxifera) (Wägele, 1989).

Terrestrial representatives of Isopoda (Oniscidea) are not an ingroup of Cymothoida, and the herein studied fossils differ from terrestrial forms in many aspects. In oniscideans the number of antennulae elements is reduced (Tabacaru and Danielopol, 1996), the mandibular palp is absent (Tabacaru and Danielopol, 1996), the border between tergites and coxal plates is usually indistinct (Gruner, 1954), and the endopod of the uropods is rod-shaped (Wägele, 1989; Broly *et al.*, 2013).

The interpretation of the herein described fossils can be further narrowed down by ruling out ingroups of Cymothoida – the narrowest group to which the herein described fossils could be determined, using apomorphic character states that are visible in the fossils ('basal delimitation of the systematic interpretation'). Some ingroups of Cymothoida can be ruled out, as they have apomorphic states where the herein described fossils have plesiomorphic character states ('distal delimitation of the systematic interpretation'). This second step of the systematic interpretation can contribute to a better understanding of the palaeoecology of the herein described fossils.

The relationship between the different lineages within Cymothoida is far from being fully understood. This way, many different ingroups of Cymothoida need to be considered. To limit the length of this section, only a selection cymothoidan lineages is discussed here. A more complete comparison between the herein described fossils and the different ingroups of Cymothoida can be found in Tab. S1.

Representatives of the groups Gnathiidae and Protognathia can be distinguished from the herein described fossils because, in Gnathiidae and Protognathia, the appendages on the trunk segment seven are absent (possibly an extreme post-displacement of their development, *cf.* manca stage; Wägele and Brandt, 1988; Wägele, 1989).

Representatives of Corallanidae, Aegidae and Cymothoidae (fish parasites) and Epicaridea (mostly crustacean parasites) can be distinguished from the herein described fossils because in those groups the dactylus is firmly conjoined with its claw, forming a hook-like compound structure (prehensile condition, Fig. 8C, dactylus). In Cymothoidae this applies for trunk appendages 1–7, in Aegidae this applies for trunk appendages 1–3, and in Corallanidae this applies at least for trunk appendage 1 (Wägele, 1989; Nagler *et al.*, 2017). This is in contrast to the herein described fossil (Fig. 8A dactylus), where the separation between the dactylus and its claw is clearly visible (*e.g.*, Figs. 3C, D, 4C).

Representatives of the group Tridentella (= Tridentellidae) can be distinguished from the herein described fossils, because the maxilliped endite is elongated and extends at least to the level of the third element of the maxilliped palp (Wägele, 1989; Bruce, 2008), whereas this is not the case in the herein described fossils (Fig. 3A, C).

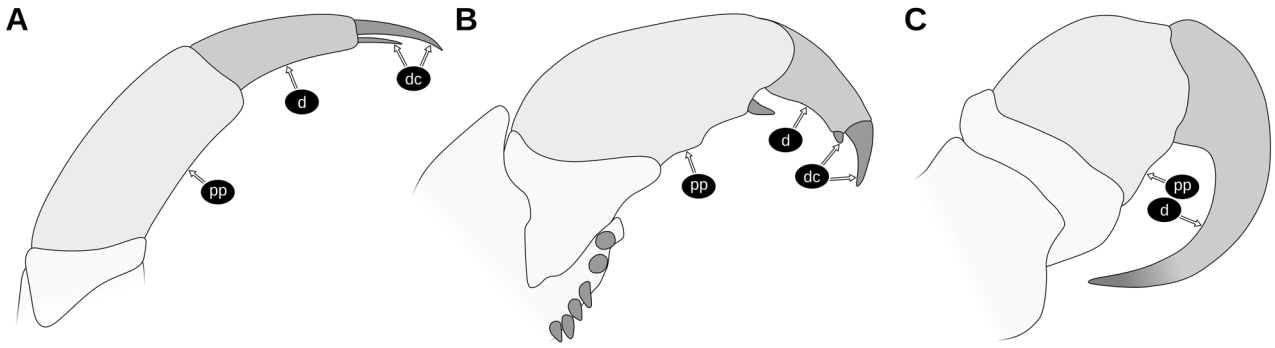

Figure 8. Comparison of the distal part of trunk appendage 1 in different lineages of Cymothoida. **A**: *Electrolana madelineae* n. sp., schematic reconstruction; **B**: *Cirolana australiense* Hale, 1925, redrawn from Bruce (1986, fig. 114L); **C**: *Elthusa vulgaris* (Stimpson, 1857), drawn after van der Wal and Haug (2020, fig. 16B). d, dactylus, dc, claws of dactylus, pp, propodus.

Well preserved fossils of the group Urda show clear morphological features that can be attributed to a parasitic lifestyle (dactylus and claw of trunk appendages 1–7 strongly curved and hook-like) (Nagler *et al.*, 2017). In Urda, aside from the morphology of the appendages, the tergites of the anterior trunk are proportionally much longer than the corresponding tergites of the pleon (Stolley, 1910).

Most of the remainder lineages of Cymothoida are collectively referred to as Cirolanidae. Representatives of Cirolanidae are characterised by an overall plesiomorphic appearance (Wägele, 1989). Brandt and Poore (2003) argued that Cirolanidae could be characterised by apomorphic characters of the mandible (tridentate incisor with the posterior tooth the most prominent and mandible spine row on a fleshy lobe); however, one of these putative apomorphic character states (tridentate incisor with the posterior tooth the most prominent) can also be found in Corallanidae (see figures in Delaney, 1989). These characters of the mouthparts, however, are very prone to become unrecognisable in the course of further specialization of the mouthparts. For the parasitic lineages of Cymothoidae – which are well characterized by their specialised mouthparts — a cirolanid-like, scavenging ancestor has been reconstructed (Menzies *et al.*, 1955; Brusca, 1981; Dreyer and Wägele, 2001). This way — even if the extant, non-parasitic, representatives of Cymothoida form a monophylum (Cirolanidae) — fossils with a cirolanid-like morphology must not necessarily belong to Cirolanidae.

Palaega is a 'form genus' (assemblage based on rough similarity) that likely comprises many different Isopoda lineages (Feldmann and Rust, 2006). Palaega is largely synonymous with Bathynomus (Wieder and Feldmann, 1989; Feldmann, 1990; Martin and Kuck, 1990; Hyžný *et al.*, 2019). Individual Cretaceous species that have been assigned to Palaega are discussed below regarding a possible conspecificity with the herein described fossils. Representatives of Bathynomus can be distinguished from the herein described fossils, because in Bathynomus the posterior margin of the pleotelson has a characteristic serration (Bruce, 1986).

Representatives of the group Pseudopalaega Mezzalira and Martins-Neto, 1992 can be distinguished from the herein described fossils, because representatives of Pseudopalaega have a strongly dorsoventrally-flattened, oval body and prominent, laterally-projecting coxal plates.

The herein described fossils resemble representatives of Natatolana in having relatively broad basipods in trunk appendages 5–7. Representatives of Natatolana can be distinguished from the herein described fossils, because in Natatolana the basipod of trunk appendage 7 is broader in its distal half and has plumose setae on the anterior margin as well as at the postero-distal angle (Keable, 2006).

The herein described fossils resemble representatives of Metacirolana in the overall morphology; however, in Metacirolana the clypeus forms a ventrally projected blade (Bruce, 1986; Sidabalok and Bruce, 2018). In the larger herein described specimen

this character is not visible; in the smaller specimen the clypeus is not projected (Fig. 3A–E). Yet, this is uninformative, as we could not find information whether this character is present in extant manca stage individuals of Metacirolana.

The groups Aatolana, Pseudolana, Plakolana, Odysseylana, Neocirolana, Eurylana, Baharilana, and Cirolana cannot securely be ruled out from the systematic interpretation of the herein described fossils and each of the groups might potentially include the fossils at hand. The fossils could, however, also belong to a different lineage within Cymothoida that has no extant representatives.

Brunnaega tomhurleyi Wilson, 2011 is very similar to the herein described fossils and could potentially be closely related. At this point it needs to be pointed out that the name Brunnaega is based on the "shared anatomical similarity" between *Brunnaega tomhurleyi* and *Brunnaega roeperi* Polz, 2005 (Wilson *et al.*, 2011: 1056) — consequently, Brunnaega should not be treated as a systematic group (see also Hyžný *et al.*, 2013).

Species delimitation

All representatives of Isopoda that have been formally described from Burmese amber are terrestrial forms (Oniscidea) (Broly *et al.*, 2015; Poinar, 2018; Ross, 2019). Recently, some specimens that are syn-inclusions to an ammonite, have been presented, including remains of presumed non-oniscidean representatives of Isopoda (Yu *et al.*, 2018). However, the limited information from the provided microscopic images is not sufficient to give precise systematic interpretations. Also, the specimens presented in Yu *et al.* (2018) do not morphologically resemble the herein presented specimens in many aspects.

Burmese amber is of earliest Late Cretaceous age (Shi *et al.*, 2012; Yu *et al.*, 2018). To limit the discussion about potential conspecificities to a reasonable set of species we only considered species with records from the Cretaceous; this includes occurrences that are *ca.* 45 million years older and 32 million years younger. To further limit the length of this section, not all of the Cretaceous species are discussed below — for a comparison of the herein describe fossils with the remainder species, see Tab. S2.

As discussed above, *B. tomhurleyi* is very similar to the herein described fossils. Yet, *B. tomhurleyi* can be distinguished from the herein described fossils, because in *B. tomhurleyi* the lateral sides of the tergites of pleon segment 1 and 5 are each concealed by the tergites of the respective preceding segment.

Cymatoga jazykowii von Eichwald, 1863 from the Cretaceous of Uljanowsk (Volga Federal District, Russia) has never been figured. The description raises doubts, whether it even is a fossil representative of Isopoda at all — it states that there are 8 or 9 segments of the anterior trunk (von Eichwald, 1863).

Cirolana cottreaui (Roger, 1946) has a trapezoid pleotelson (posteriorly truncated), whereas in the fossils at hand the pleotelson is half-oval in shape and not truncated.

In *Cirolana enigma* Wieder and Feldman, 1992 the anterior margin of the pleotelson is distinctly convex, which is not the case for the fossils at hand.

Cirolana garassinoi Feldmann, 2009 has relatively large uropods and the uropod endopods are very broad on the distal side (their distal margins are almost straight). In the fossils at hand the uropods are not that large and the broadest level of the uropod endopods is much closer to the proximal side.

Natatolana poblana Vega and Bruce, 2019 is not easy to differentiate from the herein described specimens due to preservation of the *N. poblana* types. All of the *N. poblana* types have a relatively more acute pleotelson posterior margin when compared to the larger specimen at hand. The smaller specimen at hand is similar to the *N. poblana* types, yet there is considerable size variation in the figured specimens (at least 35%, measured by pleotelson length), but not much variance in the shape of the posterior margin of the pleotelson, suggesting that young individuals of *N. poblana* also do not have a pleotelson morphology as in the fossils at hand. In addition to the small morphological differences it has to be considered that the type occurrence of *N. poblana* is *ca.* 30 million years older than Burmese amber and also remote from a palaeogeographical point of view. The affinity of *N. poblana* to the group Natatolana is questionable, as

the apomorphic characters of Natatolana as listed in Keable (2006) are not visible or not even preserved in the types of *N. poblana*.

Cymothoidana websteri Jarzembowski *et al.*, 2014 differs from the fossils at hand in having a much more triangular shaped pleotelson, comparably large uropods and the shape of the uropod endopod (in *C. websteri* with a straight lateral margin).

Representatives of Isopoda preserved in amber

Fossils of Isopoda usually do not make up a high proportion of inclusions in amber — compared to the vast number of insect inclusions. Yet, they are known from many amber sites with each a rather low diversity when compared to other groups of Euarthropoda, such as Insecta, Araneae (spiders) and Acari (mites). By far the largest fraction of inclusions of representatives of Isopoda in amber is that of terrestrial forms (Oniscidea). A detailed list of fossil oniscideans in amber has been given in Broly *et al.* (2013). Aside from oniscideans there are aquatic larvae of epicarideans in Miocene amber from Chiapas (Mexico; Serrano-Sánchez *et al.*, 2016) and from Late Cretaceous Vendean amber (France; Néraudeau *et al.*, 2017; Schädel *et al.*, 2019b). The only record so far of a non-parasitic representative of Cymothoida ("Cirolanidae") is from Eocene Baltic amber (southern coast of Baltic sea; Weitschat *et al.*, 2002; Wichard *et al.*, 2009).

Burmese amber is Earliest Cenomanian in age, which corresponds to a numeric age of about 99 million years (Shi *et al.*, 2012). So far, only two species of Isopoda have been formally described from Burmese amber: *Myanmariscus deboiseae* Broly, Maillet and Ross, 2015 and *Palaeoarmadillo microsoma* Poinar, 2018 (Broly *et al.*, 2015; Poinar, 2018). Additionally, there is another record of Oniscidea, interpreted as a representative of Tylidae, yet without formal description (Zhang, 2017; referenced in Ross, 2019). Additionally, there have been three specimens of Isopoda figured in Yu *et al.* (2019). However, with the images that are available, it cannot be ruled out that those specimens are representatives of *P. microsoma*.

Marine animals in Burmese amber

Amber is a typical terrestrial product as it derives from tree sap. The tolerance of trees towards a moist environment is quite limited for most trees with the exception of very specialised trees, such as mangroves or swamp cypresses. Thus, for a long time, aquatic organisms preserved in amber have been explained by smaller bodies of water that frequently occur in any type of forest (streams, small pools, flooded tree holes, etc.).

In Burmese amber there are records of insect larvae with supposed aquatic lifestyles (Zhao *et al.*, 2019; Schädel *et al.*, 2020). Additionally, there are inclusions of organisms that could also be linked to a marine lifestyle, such as seed shrimps (Xing *et al.*, 2018), pholadid bivalves (Mao *et al.*, 2018; Smith and Ross, 2018), snails (Gastropoda) and an ammonite shell (Yu *et al.*, 2019). An earlier record of alleged marine snails (Yu *et al.*, 2018) is likely a product of misinterpretation (they are likely representatives of the terrestrial groups Cochlostomatidae or Diplommatinidae; M. Harzhauser, pers. comm., 2019). Along with the animals preserved within the fossilized resin, marine animals that are attached to amber pieces (sea feathers, corals and oysters; Mao *et al.*, 2018) suggest a near shore environment for the Burmese amber forest.

Palaeoecology inferred from the systematic interpretation

The plesiomorphic condition for representatives of Isopoda is to live in a marine habitat. The transition from a marine habitat to limnic habitats occurred in many lineages of Isopoda, however Oniscidea is the only group to have established a terrestrial mode of life (Wägele, 1989; Brusca and Wilson, 1991; Broly *et al.*, 2013). Despite the preservation in amber, as a terrestrial substance (see discussion below), from a systematic perspective it is unlikely, that the herein presented fossils were terrestrial organisms.

Limnic habitats are inhabited by many lineages of Cymothoida, also including the parasitic lineages within the group such as Cymothoidae (Brusca, 1981) and Epicaridea (Chopra, 1923). Many representatives of ingroups of Cymothoida with plesiomorphic feeding strategies (Cirolanidae) such as Eurydice,

Pseudolana, Cirolana, Anopsilana, Hansenolana, and Natatolana live in estuarine environments (Bruce, 1986); even mangrove muds are inhabited by cymothoidans (*e.g.*, Limicolana; Bruce, 1986). There are also true freshwater species among non-parasitic cymothoidans, with probably more than one lineage being linked to ground water and cave systems (Bruce, 1986; Wägele, 1989). In conclusion, it is likely that the herein presented fossil specimens once lived in a marine or brackish environment. However, the systematic position of the fossils alone cannot provide much certainty in this regard, as the ecology of extant species is so diverse.

Functional morphology

Dense rows of long setae on pleopods, uropods and pleotelson such as those in the here described specimens are frequent among aquatic representatives of Isopoda — yet not in terrestrial forms. This might be due to the different respiratory function of the pleopods in oniscideans (Wägele, 1989). Also, setae increase the surface area of body parts, which is crucial for efficient propulsion by stroking motions of movable body parts. In the case of the pleopods and the pleotelson, increasing the surface area with dense rows of setae is seen in many aquatic species (*e.g.*, Bruce, 1986); this would however probably be disadvantageous in a terrestrial environment, because this could result in an increased adhesion of moist particles to the animal. The same applies for the wide second leg element (basipod) in trunk appendages 5–7 in the herein described fossils (Fig. 4D). Such widened basipods often occur in swimming species, *e.g.*, in the group Natatolana, but also in many species of Cirolana. In representatives of Natatolana and Politolana the basipod of the more posterior appendages of the anterior trunk is additionally equipped with long setae (Kensley and Schotte, 1989), which are not apparent in the fossils at hand (*cf.* Fig. 4D).

The morphology of the antennal flagellum in the fossils at hand, with many small elements and short setae on the ventral side, is very similar to the morphology in many aquatic cymothoidans (*cf.* figures in Bruce, 1986; Brusca *et al.*, 1995). The high surface area of such types of antennulae suggests that this would be disadvantageous in terrestrial environments that oniscideans typically inhabit — *e.g.* due to the adhesion to moist objects.

Syn-inclusions

Syn-inclusions of the smaller fossil at hand (NHMW 2017/0052/0002) are various unidentifiable euarthropodan remains (Fig. S2A, B, F) and a mite that is located in very close proximity or in contact with a gas-filled bubble (Fig. S2C–E). Also, several enigmatic needle-shaped objects are present in the amber piece (Fig. S2G). These could possibly be plant hairs or setae of euarthropodans. No inclusion within this amber piece, except for the specimens of Isopoda itself, shows any specialization for a specific environment or could be identified to a systematic level that would allow palaeoecological conclusions to be drawn.

Syn-inclusions of the larger fossil at hand (NHMW 2017/0052/0001) are an adult midge (*cf.* Psychodidae; Fig. S3A, B), an adult fly (Alavesia; V. Baranov, pers. comm., 2019; Fig. S3C, D), a beetle (Coleoptera; Fig. S3D, E), various unidentified euarthropodan remains (Fig. S4A–D) and three seed shrimp specimens (Fig. S4E–G).

The group Alavesia (Diptera: Atelestidae) has so far only been recorded from Burmese amber with one, not (yet) formally described, species (Grimaldi *et al.*, 2002). Extant species of Alavesia have been found at an ephemerous river in proximity to pools of standing water (Sinclair and Kirk-Spriggs, 2010). The larvae, even of the extant representatives of Atelestidae, are unknown and the adults are assumed to feed on flowering plants (Sinclair and Kirk-Spriggs, 2010; Sinclair, 2017). Thus, the value of the Alavesia specimen for ecological reconstruction is very limited.

The presumed psychodid specimen resembles *Bamara groehni* Stebner *et al.*, 2015 in many aspects; but especially the claspers (male genitalia) differ distinctly. The phylogenetic interpretation of the specimen in this study (and even that of *B. groehni*) is too broad to draw any ecological conclusions, as the eligible extant relatives are ecologically very diverse. The only other non-parasitic representative of Cymothoida which is preserved in amber, is from the Eocene Baltic amber and also is accompanied by (freshwater) seed shrimps (Weitschat *et al.*, 2002).

Abiotic taphonomic indicators

The two amber pieces containing the fossils at hand have a very different macroscopic appearance (Supplementary file 1: Fig. S1A). The amber piece containing the smaller specimen (NHMW 2017/0052/0002) is very clear and almost devoid of impurities. The amber piece containing the larger specimen, on the other hand, is much less transparent due to a high abundance of small-scale impurities. These impurities comprise dead organic matter (plant and animal remains) as well as a distinct type of many very small spherical inclusion of reddish colour. This kind of impurity has also been reported for other Cretaceous amber sites (Girard *et al.*, 2011; 2013; Quinney *et al.*, 2015). Girard *et al.* (2011) and likely represent fossilized tree sap double emulsions (Lozano *et al.*, 2020).

Due to these impurities, a stratified build-up is apparent in the matrix of the amber piece NHMW 2017/0052/0001. Aquatic taphocoenoses are often associated with a stratified build-up of the amber matrix (Serrano-Sánchez *et al.*, 2015; Schädel *et al.*, 2019b).

The stratification within the amber piece containing the larger specimen (NHMW 2017/0052/0001) also affects the arrangement of bubbles (Fig. 9). A large fraction of bubbles within the amber piece is confined to a narrow layer, in alignment with the stratification pattern. The content of the bubbles in the layer has the same x-ray contrast as the air outside the amber piece (Fig. S1B, C), leading to the interpretation that these bubbles are gas filled to the time of observation. The presence of crystals (presumably pyrite) within many of the bubbles, that make up the dense layer, renders it unlikely that the bubbles were gas filled to the time the resin was still fluid (although re-sublimation cannot be ruled-out entirely). Inclusions of water — often alongside with a gas phase — occur in various amber deposits (Ross, 1997; 1998; Poinar *et al.*, 1999), including Burmese amber (see fig. 1 in Caterino and Maddison, 2018). From Baltic amber there is even a record of a seed shrimp (Ostracoda) embedded in a water filled bubble (Keyser and Weitschat, 2005). The circumstances under which such abiotic inclusions form are still poorly studied. Experiments on synthetic resins have shown that resins are permeable to water (Hashimoto *et al.*, 2005). For fossil natural resins permeability has been shown for gases, and permeability for fluids is also suggested (Hopfenberg *et al.*, 1988 and references therein). Cases of extreme dehydration (mummification) within Baltic amber that allowed for ultrastructure preservation have been explained to be the result of the absorption of water by terpenes and/or saccharides within the resin (Poinar and Hess, 1982).

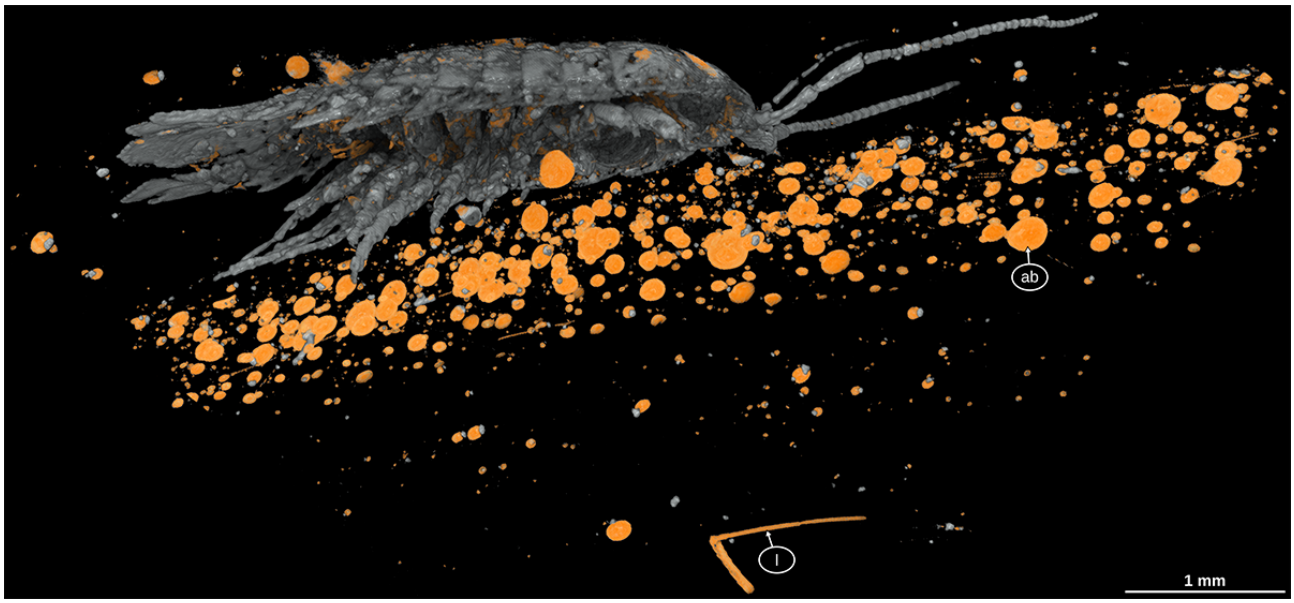

Figure 9. Holotype of *Electrolana madelineae* sp. nov. (NHMW 2017/0052/0001), habitus in ventrolateral view and surrounding objects in the resin, volume rendering image, two different transfer functions and clipping planes applied, orange colour transfer function solely depicts extremely low-x-ray contrast areas (gas phase). ab, air bubble; l, leg, Euarthropoda.

From the micro-CT scan it becomes apparent that a mineral with high x-ray contrast is present in the body cavities of the larger fossil at hand and in gas filled bubbles surrounding it (Fig. S1B, C). Pyrite is an iron sulfide (FeS_2) with cubic (= isometric) crystals that would match the structures seen in the micro-CT scan. Pyrite is a common mineral in sedimentary environments and is formed by bacterial activity in chemically reducing conditions. The presence of enough sulfate ions (SO_4^{2-}) in the water of the environment is a prerequisite for the formation of pyrite (Knight *et al.*, 2010) and can be provided, for example, by nearby gypsum deposits. The crystals do not penetrate the surface of the fossil. Thus, this kind of preservation can be interpreted as an incomplete pseudomorph of pyrite after the fossil arthropod (pyrite casting the shape of the fossil organisms). Pseudomorphs of pyrite after fossils are a common phenomenon but are usually known from hard-shelled marine animals such as ammonites (Hudson, 1982) but have also been reported for amber inclusions (Knight *et al.*, 2010). Pyrite is not uncommon in Burmese amber and has been interpreted as an indicator for the presence of sulfate rich water before (Schlüter, 1978; Smith and Ross, 2018). Pyrite is also present in other supposedly aquatic taphocoenoses in amber (Serrano-Sánchez *et al.*, 2015; 2016; Smith and Ross, 2018).

There is a bubble-like object with a similarly high radiometric density as the presumed pyrite crystals (Figs. 5B, C, S1C, D). However, it lacks apparent crystal structures, and therefore its nature and cause remains unexplained. Similar structures have been found associated with burrowing bivalves (Pholadidae) in Burmese amber. Spectrometric tests have revealed that those cavities are filled with carbonate-rich material (Smith and Ross, 2018).

A reasonable interpretation of the taphonomic situation in the amber piece NHMW 2017/0052/0001 is that resin was recurrently released into a body of water, causing a stratification and the entrapment of water between two layers of resin flow. The entrapped water formed bubbles within the still fluid resin. Subsequently, the water permeated out of the resin. This latter process could have happened well after the resin polymerized and formed amber.

Preservation of aquatic organisms in amber

In most amber sites, organisms with a supposed aquatic lifestyle are extremely rare in comparison to terrestrial organisms. This does not necessarily apply for adults of organisms with aquatic larvae.

Typical interpretations of the preservation of aquatic organisms in fossil resins include dead and dried up specimens being transported to the resin by wind (Weitschat *et al.*, 2002) or still hydrated specimens being transported by spray (Schmidt *et al.*, 2018).

The herein presented specimens show no signs of desiccation, such as collapsed fine structures in areas of the body that are less sclerotized. Also, the fossils are very complete, *i.e.*, no delicate structures such as flagellum articles of the antenna are missing. This suggests, that the individuals were not exposed to desiccation or strong mechanical forces (*e.g.*, transport by spray).

Experiments in a modern day swamp have shown that resin, when submerged in water, stays fluid for a long time (reduced evaporation of volatiles) and aquatic animals can be caught in still-fluid submerged resin by autonomous movement (Schmidt and Dilcher, 2007). This process is also the best explanation for some instances found in Campo La Granja (Chiapas) amber, where, for example, traces of torn-off side-swimmer (Amphipoda) legs have been found. Such an arrangement is only possible when the side-swimmers were still alive when they got embedded in the resin (Serrano-Sánchez *et al.*, 2015). Similar explanations have been given for microorganisms preserved in amber (Waggoner, 1994).

In close proximity to the larger specimen (NHMW 2017/0052/0001) three seed shrimps (Ostracoda) are preserved. The larger specimen and the seed shrimps are all on one side of the above mentioned layer of bubbles whereas the much larger side of the amber piece is devoid of seed shrimps or other organisms for which an aquatic environment can be reconstructed. This high abundance in a small volume of amber also points towards an *in situ* entrapment rather than towards a transport of aquatic organisms by wind or spray.

With several different aquatic organisms preserved in Burmese amber (Mao *et al.*, 2018; Smith and Ross,

2018; Xing *et al.*, 2018; Yu *et al.*, 2019), including marine ones, it appears to be the most consistent interpretation that the forest that produced the fossilised resin was close to a marine environment and at least parts of the forest were flooded temporarily.

Fossil record of early developmental stages in Isopoda

Most representatives of Isopoda have hatchlings that are very similar in their outer morphology to the corresponding adults (Boyko and Wolff, 2014), at least at first sight. Consequently, it is very difficult to identify whether a fossil specimen is of a very early stage of development or a small adult. Yet, there are two factors, which sometimes allow for a better identification of the individual developmental stage of a fossil representative of Isopoda: (1) The so-called manca stage is characterized by the absence of well-developed legs on trunk segment 7 (postocular segment 13; Boyko and Wolff, 2014). Before the individual becomes adult, within a single moult, a well-developed leg appears at this segment (Boyko and Wolff, 2014). The resulting, not yet adult, individuals are often termed 'juveniles' (Boyko and Wolff, 2014). The fossil record of manca stage individuals is very sparse. The smaller specimen presented in this study (Fig. 10A) represents only the second fossil record of this life stage that can undoubtedly be identified as such. The other record is from terrestrial representatives of Isopoda (Oniscidea) in Miocene Mexican amber (Fig. 10B) (Broly *et al.*, 2017). From Burmese amber there is also another short note on presumable hatchlings of terrestrial representatives of Isopoda (Poinar, 2018); however, the quality of the illustration does not allow to reliably evaluating this observation. (2) Within Epicaridea, which itself is an ingroup of Cymothoida, a developmental pattern had secondarily evolved, resulting in (true) larvae that are distinct from the corresponding adults (see discussion in Haug, 2020). Fossil larvae of Epicaridea have been found in two amber sites. One record is from the Cretaceous of France, with multiple specimens likely corresponding to a single species (Fig. 10C; Schädel *et al.*, 2019b). The other record is from the Miocene of Mexico with several specimens that likely correspond to different species (Fig. 10D–H) (Serrano-Sánchez *et al.*, 2016).

Taxonomy

Euarthropoda (*sensu* Walossek, 1999)

Eucrustacea (*sensu* Walossek, 1999)

Peracarida Calman, 1904

Isopoda Latreille, 1817

Scutocoxifera Dreyer and Wägele, 2002

Cymothoida Wägele, 1989

***Electrolana* gen. nov.**

Zoobank: urn:lsid:zoobank.org:act:D069AD30-5BE0-44DB-B436-4A04B7FE8CDF

Etymology. Latinized spelling of the Greek word ḗlektron for amber with the suffix *-lana*, originating from the name Cirolana.

Remarks. The name *Electrolana* gen. nov. is erected to provide a binomial name for the species below. Since only one species will be included as of this study, no diagnosis can be given.

***Electrolana madelineae* sp. nov.**
Figs. 2–6, 7A, 8A, 9, 10A, S1, S6–8

Zoobank: urn:lsid:zoobank.org:act:8D1A3CC8-B700-4819-85A9-4ACBA02966D0

Etymology. After Madeline Pankowski of Rockville, Maryland, USA, daughter of Mark Pankowski who donated the types to the Museum of Natural History in Vienna.

Material examined. Holotype: NHMW 2017/0052/0001, Natural History Museum Vienna. Paratype: NHMW 2017/0052/0002, Natural History Museum Vienna.

Ontogenetic stage of the type. The paratype is of a manca stage; the holotype is a post-manca juvenile or an adult.

Type locality. Near Noje Bum, Hukawng Valley, Kachin State, Myanmar.

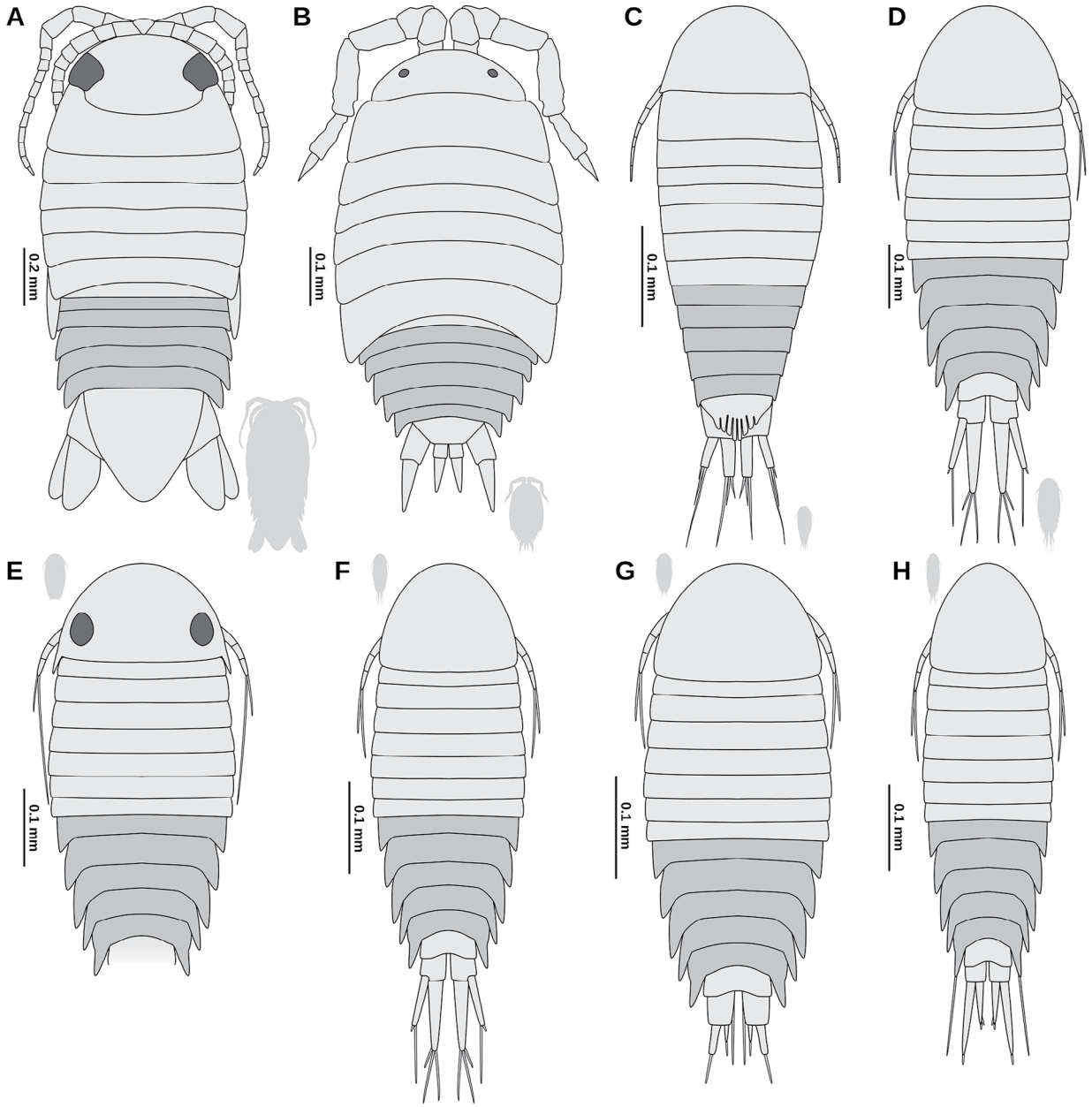

Figure 10. Graphical summary of all known manca-stage or larval fossils of Isopoda, reconstruction line drawings, free pleon tergites (postocular segments 14–18) in darker grey. **A.** Paratype of *Electrolana madelineae* sp. nov. (NHMW 2017/0052/0002); **B**: *Aquitanoscia chiapasensis* Broly *et al.*, 2017; **C**: *Vacuotheca dupeorum* Schädel *et al.*, 2019b; **D**: IHNFG-4951-Ep1 ('specimen 2') Serrano Sanchez *et al.* (2016); **E**: openstreetmap.org IHNFG-4964-Ep2 ('specimen 5b') Serrano Sanchez *et al.* (2016); **F**: IHNFG-5321-Ep1 ('specimen 6') Serrano Sanchez *et al.* (2016); **G**: IHNFG-4971-Ep1 ('specimen 3') Serrano Sanchez *et al.* (2016); **H**: IHNFG-4939-Ep1 ('specimen 1') Serrano Sanchez *et al.* (2016).

Type stratum. Unknown stratum, 98.8 million years, earliest Cenomanian, earliest Late Cretaceous, after Shi *et al.* (2012).

Differential diagnosis. Body drop shaped in dorsal view, tapering posteriorly, about 2.5 to 2.2 times longer than wide; tergite of trunk segment 1 about twice as long as succeeding segments; dactylus and claws of trunk appendages 1–3 gently curved inwards, not hook-like; coxal plates well developed, triangular in trunk segments 4–7 (postocular segments 10–13); basipod of trunk appendage 6 broad, posterior margin convex, median ridge along the mid-line of the lateral surface; coxal plate of trunk segment 7 (postocular segment 13) very conspicuous in dorsal view, extending distally to the level of pleon segment 5;

tergites of pleon segments 1–5 (postocular segments 14–18) free; tergite of pleon segment 1 (postocular segment 14) short, laterally covered by the tergite of trunk segment 7 (postocular segment 13); basipod of pleopod 1 (postocular segment 14) wider than long; pleopod 1 not operculate, concealing the succeeding pleopods; tergite of pleon segment 5 (postocular segment 18) with free lateral margins, not covered by the tergite of the preceding segment; endopod of pleopod 5 (postocular segment 18) more slender than the corresponding exopod, no setae on the distal margin; pleotelson half-oval in shape, slightly longer than wide, straight anterior margin, without distinct ornamentation on the dorsal surface, posterior margin without large spines, posterior margin with numerous setae grouped in the posterior-most part; uropod endopod about twice as long as wide, with median angle, not 'truncated'.

Remarks on the differential diagnosis. Due to the limited set of characters available, using the current methods, this diagnosis will not be able to differentiate the new species from all fossil or extant species. Thus, this differential diagnosis should be seen as a short recap of the description with respect to the discussion above.

Systematic interpretation. Cymothoida *incertae sedis*, *nec* Anuropus, *nec* Tridentella, *nec* Corallanidae, *nec* Aegidae, *nec* Cymothoidae, *nec* Epicaridea, *nec* Gnathiidae, *nec* Protognathia, *nec* Urda, *nec* Bathynomus, *nec* Colopisthus, *nec* Boorlana, *nec* Parabathynomus, *nec* Bahalana, *nec* Arubolana, *nec* Cirolanides, *nec* Typhlocirolana, *nec* Turcolana, *nec* Speocirolana, *nec* Sphaeromides, *nec* Skotobaena, *nec* Sphaerolana, *nec* Atarbolana, *nec* Aphantolana, *nec* Annina, *nec* Pseudaega, *nec* Politolana, *nec* Oncilorpheus, *nec* Natatolana, *nec* Haptolana, *nec* Excirolana, *nec* Eurydice, *nec* Conilera, *nec* Dolicholana. The following extant ingroups of Cymothoida represent likely affinities for *Electrolana madelineae* sp. nov.: Aatolana, Pseudolana, Plakolana, Odysseylana, Neocirolana, Eurylana, Baharilana, and Cirolana.

Remarks on the systematic interpretation. The Latin term *nec* (= but not) is used to list ingroups of Cymothoida, to which *Electrolana madelineae* sp. nov. does not belong (as applied in Schädel *et al.*, 2019a).

Conclusion

The two herein presented specimens are interpreted as conspecific and represent different stages of individual development. The smaller specimen thus could be identified as a manca stage. The specimens represent a not previously described species, due to distinct morphological differences and the huge temporal distance to species with similar morphological features. An affinity to parasitic lineages within Cymothoida, which is the narrowest group to which the fossil specimens could be identified, could be excluded due to the visible absence of apomorphies of the parasitic ingroups. Both the systematic interpretation of the fossils themselves, as well as the surrounding taphonomic condition in one of the amber pieces (*e.g.*, seed shrimp syninclusions) suggest that at least one of the specimens became embedded in resin while submerged in water. The complete taphocoenoses suggest the presence of a water body in proximity to the resin producing tree but not necessarily brackish or marine conditions within this water body.

Acknowledgements

This study would not have been possible without Mark Pankowski (Rockville, Maryland, USA) who obtained the amber pieces and reached out to us to study them. He donated the amber pieces to the Natural History Museum Vienna to make this study possible. Niel Bruce (North West University, South Africa) helped us to prepare this manuscript by sharing his expertise and providing valuable constructive criticism. Mathias Harzhauser (Natural History Museum Vienna) is to be thanked for access to the specimens and helpful comments on the manuscript. We thank Roland Melzer (Zoological State Collection, Munich) for his help with the micro-CT scans. We thank C. Haug and J.M. Starck (both Munich) for their long-standing support. We thank Francisco Vega (Mexico City), Evin P. Maguire (Kent State University) and one anonymous reviewer for their encouraging and helpful comments on the manuscript. The project was kindly funded by the Deutsche Forschungsgemeinschaft (DFG Ha 6300/3-2). J.T. Haug is kindly funded by the Volkswagen Foundation

(Lichtenberg professorship). The research of MH was supported by VEGA 02/0136/15 and APVV-17-0555. Except for hardware related software, this manuscript was entirely prepared, using free and open software – we warmly appreciate the effort of those who made this possible.

Supplementary Material

Supplementary file 1: Figure S1. A: overview image of the two amber pieces photographed under the same light settings, white light microscopy, 50x (VHX); **B:** holotype of *Electrolana madelineae* sp. nov. (NHMW 2017/0052/0001), cross section through the anterior trunk region, micro-CT image, reconstructed slice; **C**: holotype of *Electrolana madelineae* sp. nov. (NHMW 2017/0052/0001), cross section through the anterior trunk region, micro-CT image, reconstructed slice; **D**: holotype of *Electrolana madelineae* sp. nov. (NHMW 2017/0052/0001), head region in frontal view, red-cyan stereo anaglyph, volume rendering images based on micro-CT data. a, antenna; al, antennula; ab, air bubble; ap, air phase; fl, frontal lamina; py, pyrite; ?, unknown material forming an irregular bubble. https://doi.org/10.20363/mdb.u254_m-26.1

Supplementary file 2: Figure S2. Syn-inclusions of the paratype of *Electrolana madelineae* sp. nov. (NHMW 2017/0052/0002). **A**: Isolated leg, Euarthropoda , white light microscopy, 500x (VHX); **B**: isolated distal element of leg, Euarthropoda, white light microscopy, 500x (VHX); **C–E**: mite (Arachnida: Acari) in ventral view. **C:** white light microscopy, 300x (VHX); **D**: transmitted light microscopy, 20x (BZ); **E**: epifluorescence microscopy, 20x (BZ); **F**: possible cuticle remains, Euarthropoda, white light microscopy, 150x (VHX); **G**: multiple needle-like objects, possibly plant hairs or setae of euarthropodans, white light microscopy, 500x (VHX). https://doi.org/10.20363/mdb.u254_m-25.1

Supplementary file 3: Figure S3. Syn-inclusions of the holotype of *Electrolana madelineae* sp. nov. (NHMW 2017/0052/0001). **A, B**: Diptera *cf.* Psychodidae, habitus in ventral view, different illuminations, white light microscopy, 200x (VHX); **C, D**: *cf. Alavesia* (Empidoidea: Atelestidae), **C**: dorso-lateral view, white light microscopy, 100x (VHX), **D**: ventro-lateral view, white light microscopy, 100x (VHX); **E, F**: beetle (Coleoptera), **E**: antero-dorsal view, white light microscopy, 200x (VHX), **F**: postero-ventral view, white light microscopy, 200x (VHX). https://doi.org/10.20363/mdb.u254_m-24.1

Supplementary file 4: Figure S4. Syn-inclusions of the holotype of *Electrolana madelineae* sp. nov. (NHMW 2017/0052/0001). **A**: remains, Euarthropoda, white light microscopy, 100x (VHX); **B**: two isolated but closely grouped legs, Euarthropoda, white light microscopy, 200x (VHX); **C**: detail of the upper leg from B, white light microscopy, 200x (VHX); **D**: isolated leg, Euarthropoda, white light microscopy, 100x (VHX); **E–G**: Ostracoda, three different specimens, white light microscopy, **E**: 200x (VHX), **F**: 500x (VHX), **G**: 300x (VHX).

https://doi.org/10.20363/mdb.u254_m-23.1

Supplementary file 5: Table S1. Morphological comparison between *Electrolana madelineae* sp. nov. and systematic groups within Scutocoxifera (Isopoda; Gruner, 1954; Ferrara and Lanza, 1978; Jansen, 1978; Bruce, 1981; 1986; 1994; 2008; Wägele and Brandt, 1988; Javed and Yasmeen, 1989; Wägele, 1989; Schotte, 1994; Brusca *et al.*, 1995; George and Longerbeam, 1997; Keable, 1998; 1999; 2006; Bruce and Olesen, 2002; Riseman and Brusca, 2002; Brandt and Poore, 2003; Bruce and Svavarsson, 2003; Moore and Brusca, 2003; Wilson, 2003; Wilson *et al.*, 2011; Jones and Nithyanandan, 2012; Paiva and Souza-Filho, 2015; Nagler *et al.*, 2017; Sidabalok and Bruce, 2018). Use the UTF-8 character encoding and commas as the only delimiters to open the file. https://doi.org/10.20363/mdb.u254_m-22.1

Supplementary file 6: Table S2. Morphological comparison between *Electrolana madelineae* sp. nov. and isopod species with occurrences in the Cretaceous (von Eichwald, 1863; Woodward, 1870; Stolley, 1910; Rathbun, 1935; Malzahn, 1968; Bowman, 1971; Spassky and Kravtsov, 1976; Wieder and Feldmann, 1992; Calzada and Gómez Pallerola, 1994; Fraaye and Summesberger, 1999; Feldmann and Goolaerts, 2005; Karasawa *et al.*, 2008; Feldmann, 2009; Feldmann and Charbonnier, 2011; Wilson *et al.*, 2011; Jarzembowski *et al.*, 2014; Vega *et al.*, 2019). Use the UTF-8 character encoding and commas as the only delimiters to

open the file. https://www.doi.org/10.20363/mdb.u254_m-21.1

Supplementary file 7: Figure S5. Reconstructed micro-CT-scan data in form of a stack of images (Tagged Image Format, TIF). https://doi.org/10.20363/mdb.u254_m-27.1

Supplementary file 8: Figure S6. Paratype of *Electrolana madelineae* sp. nov. (NHMW 2017/0052/0002), habitus in dorsal view, white light microscopy, 200x (VHX), stereo pair for parallel viewing. https://www.morphdbase.de/?M_Schaedel_20200502-M-29.1

Supplementary file 9: Figure S7. Paratype of *Electrolana madelineae* sp. nov. (NHMW 2017/0052/0002), head region in antero-dorsal view, white light microscopy, 200x (VHX), stereo pair for parallel viewing. https://www.morphdbase.de/?M_Schaedel_20200502-M-28.1

Supplementary file 10: Figure S8. Paratype of *Electrolana madelineae* sp. nov. (NHMW 2017/0052/0002), habitus in ventral view, white light microscopy, 200x, stereo pair for parallel viewing. https://www.morphdbase.de/?M_Schaedel_20200502-M-30.1

References

Anderson, G. and Dale, W.E. 1981. *Probopyrus pandalicola* (Packard) (Isopoda, Epicaridea): morphology and development of larvae in culture. *Crustaceana*, 41: 143–161.

Ax, P. 2000. The Phylogenetic System of the Metazoa. Multicellular Animals, Vol. 1. Berlin, Springer-Verlag, 154p.

Bowman, T.E. 1971. *Palaega lamnae*, new species (Crustacea: Isopoda) from the Upper Cretaceous of Texas. *Journal of Paleontology*, 45: 540–541.

Boyko, C.B. and Wolff, C. 2014. Isopoda and Tanaidacea. p. 210–212. In: J.W. Martin, J. Olesen, and J.T. Hoeg (eds), Atlas of crustacean Larvae. Baltimore, Johns Hopkins University Press.

Brandt, A. and Poore, G.C. 2003. Higher classification of the flabelliferan and related Isopoda based on a reappraisal of relationships. *Invertebrate Systematics*, 17: 893–923.

Broly, P.; Deville, P. and Maillet, S. 2013. The origin of terrestrial isopods (Crustacea: Isopoda: Oniscidea). *Evolutionary Ecology*, 27: 461–476.

Broly, P.; Maillet, S. and Ross, A.J. 2015. The first terrestrial isopod (Crustacea: Isopoda: Oniscidea) from Cretaceous Burmese amber of Myanmar. *Cretaceous Research*, 55: 220–228.

Broly, P.; Serrano-Sánchez, M. de L.; Rodríguez-García, S. and Vega, F.J. 2017. Fossil evidence of extended brood care in new Miocene Peracarida (Crustacea) from Mexico. *Journal of Systematic Palaeontology*, 15: 1037–1049.

Bruce, N. 1981. Cirolanidae (Crustacea: Isopoda) of Australia: diagnoses of *Cirolana* Leach, *Metacirolana* Nierstrasz, *Neocirolana* Hale, *Anopsilana* Paulian & Debouteville, and three new genera— *Natatolana, Politolana* and *Cartetolana*. *Marine and Freshwater Research*, 32: 945.

Bruce, N.L. 1986. Cirolanidae (Crustacea: Isopoda) of Australia. *Records of the Australian Museum, Supplement*, 6: 1–239.

Bruce, N.L. 1994. The marine isopod *Neocirolana* Hale, 1925 (Crustacea: Cirolanidae) from tropical Australian waters. *Memoirs of the Queensland Museum*, 37: 41–51.

Bruce, N.L. 2008. New species of *Tridentella* Richardson, 1905 (Isopoda: Cymothoida: Tridentellidae), tropical marine isopod crustaceans from the Banda Sea, Indonesia. *Zootaxa*, 1734: 43–58.

Bruce, N.L. and Olesen, J. 2002. Cirolanid isopods from the Andaman Sea off Phuket, Thailand, with description of two new species. *Phuket Marine Biological Center Special Publication*, 23: 109–131.

Bruce, N.L. and Svavarsson, J. 2003. A new genus and species of cirolanid isopod (Crustacea) from Zanzibar, Tanzania, western Indian Ocean. *Cahiers de Biologie Marine*, 44: 1–12.

Brusca, R.C. 1981. A monograph on the Isopoda Cymothoidae (Crustacea) of the eastern Pacific. *Zoological Journal of the Linnean Society*, 73: 117–199.

Brusca, R.C.; Coelho, V.R. and Taiti, S. 2001. Suborder Oniscidea (Terrestrial Isopods). Tree of life web project, http://tolweb.org/notes/?note_id=4179. Accessed on 4 December 2019.

Brusca, R.C.; Wetzer, R. and France, S.C. 1995. Cirolanidae (Crustacea: Isopoda: Flabellifera) of the Tropical Eastern Pacific. *Proceedings of the San Diego Society of Natural History*, 30: 1–96.

Brusca, R.C. and Wilson, G.D.F. 1991. A phylogenetic analysis of the Isopoda with some classificatory recommendations. *Memoirs of the Queensland Museum*, 31: 143–204.

Calman, W.T. 1904. XVIII.—On the classification of the Crustacea Malacostraca. *Annals and Magazine of Natural History*, 13: 144–158.

Calzada, S. and Gómez Pallerola, J.E. 1994. Un nuevo Isópod (Crustacea) de Sta. Maria de Meià. *Batalleria*, 4: 27–30.

Caterino, M.S. and Maddison, D.R. 2018. An early and mysterious histerid inquiline from Cretaceous Burmese amber (Coleoptera, Histeridae). *ZooKeys*, 733: 119–129.

Chopra, B. 1923. Bopyrid isopods parasitic on Indian Decapoda Macrura. *Records of the Indian Museum*, 25: 411–550.

Daley, A.C. and Drage, H.B. 2016. The fossil record of ecdysis, and trends in the moulting behaviour of trilobites. *Arthropod Structure & Development*, 45: 71–96.

Delaney, P.M. 1989. Phylogeny and biogeography of the marine isopod family Corallanidae (Crustacea, Isopoda, Flabellifera). *Contribution in Science, Natural History Museum of Los Angeles County*, 409: 1–75.

Dreyer, H. and Wägele, J.-W. 2001. Parasites of crustaceans (Isopoda: Bopyridae) evolved from fish parasites: molecular and morphological evidence. *Zoology*, 103: 157–178.

Dreyer, H. and Wägele, J.-W. 2002. The Scutocoxifera tax. nov. and the information content of nuclear ssu rDNA sequences for reconstruction of isopod phylogeny (Peracarida: Isopoda). *Journal of Crustacean Biology*, 22: 217–234.

Dyar, H.G. 1890. The number of molts of Lepidopterous larvae. *Psyche: A Journal of Entomology*, 5: 420–422.

Eichwald, E. von 1863. Beitrag zur nähern Kenntnis der in meiner Lethaea Rossica beschriebenen Illaenen und über einige Isopoden aus andern Formationen Russlands. *Société Impériale des Naturalistes de Moscou*, 36: 372–424.

Feldmann, R.M. 1990. Comment on the proposed precedence of *Bathynomus* A. Milne Edwards, 1879 (Crustacea, Isopoda) over Palaega Woodward, 1870. *Bulletin of Zoological Nomenclature*, 47: 290–291.

Feldmann, R.M. 2009. A new cirolanid isopod (Crustacea) from the Cretaceous of Lebanon: Dermoliths document the pre-molt condition. *Journal of Crustacean Biology*, 29: 373–378.

Feldmann, R.M. and Charbonnier, S. 2011. *Ibacus cottreaui* Roger, 1946, reassigned to the isopod genus *Cirolana* (Cymothoida: Cirolanidae). *Journal of Crustacean Biology*, 31: 317–319.

Feldmann, R.M. and Goolaerts, S. 2005. *Palaega rugosa*, a new species of fossil isopod (Crustacea) from Maastrichtian Rocks of Tunisia. *Journal of Paleontology*, 79: 1031–1035.

Feldmann, R.M. and Rust, S. 2006. *Palaega kakatahi* n. sp.: The first record of a marine fossil isopod from the Pliocene of New Zealand. *New Zealand Journal of Geology and Geophysics*, 49: 411–415.

Ferrara, F. and Lanza, B. 1978. *Skotobaena monodi* , espèce nouvelle de cirolanidé phréatobie de la Somalie (Crustacea Isopoda): (Pubblicazioni del centro di studio per la faunistica ed ecologia tropicali del c.n.r.: cxlii). *Monitore Zoologico Italiano. Supplemento*, 10: 105–112.

Fowler, G.H. 1904. Biscayan plankton collected during a cruise of H.M.S. "Research" 1900. Part xii. The Ostracoda. *Transactions of the Linnean Society of London*, 2: 219–336.

Fraaye, R.H. and Summesberger, H. 1999. New crustacean records from the Late Campanian of the Gschiefgraben (Cretaceous, Austria). *Beiträge zur Paläontologie*, 24: 1–6.

George, R.Y. and Longerbeam, A.A. 1997. Two new species of cirolanid isopod crustaceans from Onslow Bay and Hatteras Slope off North Carolina: *Eurydice bowmani* n. sp. and *Conilera menziesi* n. sp. *Journal of the Elisha Mitchell Scientific Society*, 113: 163–170.

Girard, V.; Breton, G.; Perrichot, V.; Bilotte, M.; Le Loeuff, J.; Nel, A.; Philippe, M. and Thevenard, F. 2013. The Cenomanian amber of Fourtou (Aude, Southern France): Taphonomy and palaeoecological implications. *Annales de Paléontologie*, 99: 301–315.

Girard, V.; Néraudeau, D.; Adl, S.M. and Breton, G. 2011. Protist-like inclusions in amber, as evidenced by Charentes amber. *European Journal of Protistology*, 47: 59–66.

Grimaldi, D.A.; Engel, M.S. and Nascimbene, P.C. 2002. Fossiliferous Cretaceous amber from Myanmar (Burma): its rediscovery, biotic diversity, and paleontological significance. *American Museum Novitates*, 3361: 1–71.

Gruner, H.-E. 1954. Über das Coxalglied der Pereiopoden der Isopoden (Crustacea). *Zoologischer Anzeiger*, 152: 312–317.

Hansen, T. and Hansen, J. 2010. First fossils of the isopod genus *Aega* Leach, 1815. *Journal of Paleontology*, 84: 141–147.

Hashimoto, M.; Tay, F.R.; Ito, S.; Sano, H.; Kaga, M. and Pashley, D.H. 2005. Permeability of adhesive resin films. *Journal of Biomedical Materials Research Part B: Applied Biomaterials*, 74B: 699–705.

Haug, C.; Kutschera, V.; Ahyong, S.; Vega, F.; Maas, A.; Waloszek, D. and Haug, J. 2013. Re-evaluation of the Mesozoic mantis shrimp *Ursquilla yehoachi* based on new material and the virtual peel technique. *Palaeontologia Electronica*, 16: 1–14.

Haug, C.; Mayer, G.; Kutschera, V.; Waloszek, D.; Maas, A. and Haug, J.T. 2011. Imaging and documenting Gammarideans. *International Journal of Zoology*, 2011: 1–9.

Haug, J.T. 2020. Why the term "larva" is ambiguous, or what makes a larva? *Acta Zoologica*, 101: 167–188.

Haug, J.T. 2019. Categories of developmental biology: Examples of ambiguities and how to deal with them. p. 93–102. In: G. Fusco (ed), Essays for Alessandro Minelli, Festschrift, 2. Padova, Padova University Press.

Haug, J.T.; Haug, C.; Kutschera, V.; Mayer, G.; Maas, A.; Liebau, S.; Castellani, C.; Wolfram, U.; Clarkson, E.N.K. and Waloszek, D. 2011. Autofluorescence imaging, an excellent tool for comparative morphology. *Journal of Microscopy*, 244: 259–272.

Hopfenberg, H.B.; Witchey, L.C.; Poinar, G.O.; Beck, C.W.; Chave, K.E.; Smith, S.V.; Horibe, Y. and Craig, H. 1988. Is the Air in Amber Ancient? *Science, New Series*, 241: 717–721.

Hörnig, M.K.; Sombke, A.; Haug, C.; Harzsch, S. and Haug, J.T. 2016. What nymphal morphology can tell us about parental investment – a group of cockroach hatchlings in Baltic Amber documented by a multi-method approach. *Palaeontologia Electronica*, 19: 1–20.

Hosie, A.M. 2008. Four new species and a new record of Cryptoniscoidea (Crustacea: Isopoda: Hemioniscidae and Crinoniscidae) parasitising stalked barnacles from New Zealand. *Zootaxa*, 1795: 1–28.

Hudson, J.D. 1982. Pyrite in ammonite bearing shales from the Jurassic of England and Germany. *Sedimentology*, 29: 639–667.

Hyžný, M.; Bruce, N.L. and Schlögl, J. 2013. An appraisal of the fossil record for the Cirolanidae (Malacostraca: Peracarida: Isopoda: Cymothoida), with a description of a new cirolanid isopod crustacean from the early Miocene of the Vienna Basin (Western Carpathians). *Palaeontology*, 56: 615–630.

Hyžný, M.; Pasini, G. and Garassino, A. 2019. Supergiants in Europe: on the cirolanid isopod *Bathynomus* A. Milne Edwards, 1879 (Malacostraca, Peracarida) from the Plio-Pleistocene of Italy. *Neues Jahrbuch für Geologie und Paläontologie - Abhandlungen*, 291: 283–298.

Jansen, K.P. 1978. A revision of the genus *Pseudaega* Thomson (Isopoda: Flabellifera: Cirolanidae) with diagnoses of four new species. *Journal of the Royal Society of New Zealand*, 8: 143–156.

Jarzembowski, E.A.; Wang, B.; Fang, Y. and Zhang, H. 2014. A new aquatic crustacean (Isopoda: Cymothoida) from the early Cretaceous of southern England and comparison with the Chinese and Iberian biotas. *Proceedings of the Geologists' Association*, 125: 446–451.

Javed, W. and Yasmeen, R. 1989. *Atarbolana setosa*, a new Cirolanid isopod from the Northern Arabian Sea. *Crustaceana*, 56: 78–82.

Johansen, P.-O. 2000. Contribution to the knowledge of growth and postmarsupial development of *Natatolana borealis* (Crustacea: Isopoda). *Journal of the Marine Biological Association of the United Kingdom*, 80: 623–632.

Jones, D.A. and Nithyanandan, M. 2012. Taxonomy and distribution of the genus *Eurydice* Leach, 1815 (Crustacea,

Isopoda, Cirolanidae) from the Arabian region, including three new species. *Zootaxa*, 3314: 45–57. Karasawa, H.; Ohara, M. and Kato, H. 2008. New records for Crustacea from the Arida Formation (Lower Cretaceous, Barremian) of Japan. *Boletín de la Sociedad Geológica Mexicana*, 60: 101–110.

Keable, S.J. 1998. A third species of *Aatolana* Bruce, 1993 (Crustacea: Isopoda: Cirolanidae). *Records of the Australian Museum*, 50: 19–26.

Keable, S.J. 1999. New species and records of *Plakolana* Bruce (Crustacea: Isopoda: Cirolanidae) from Australia. *Memoirs of The Queensland Museum*, 43: 763–775.

Keable, S.J. 2006. Taxonomic revision of *Natatolana* (Crustacea: Isopoda: Cirolanidae). *Records of the Australian Museum*, 58: 133–244.

Kensley, B. and Schotte, M. 1989. Guide to the marine isopod crustaceans of the Caribbean. Smithsonian Institution Pres, 308p.

Keyser, D. and Weitschat, W. 2005. First record of ostracods (Crustacea) in Baltic amber. *Hydrobiologia*, 538: 107–114.

Knight, T.K.; Bingham, P.S.; Grimaldi, D.A.; Anderson, K.; Lewis, R.D. and Savrda, C.E. 2010. A new Upper Cretaceous (Santonian) amber deposit from the Eutaw Formation of eastern Alabama, USA. *Cretaceous Research*, 31: 85–93.

Kocsis, A.T. and Raja, N.B. 2020. chronosphere: Earth system history variables (pre-release) (Version 0.3.0). Zenodo. http://doi.org/10.5281/zenodo.3525482. Accessed on 11 June 2020.

Kypke, J.L. and Solodovnikov, A. 2018. Every cloud has a silver lining: X-ray micro-CT reveals *Orsunius* rove beetle in Rovno amber from a specimen inaccessible to light microscopy. *Historical Biology*, 1–11.

Latreille, P.A. 1817. Le règne animal distribué d'après son organisation: pour servir de base a l'histoire naturelle des animaux et d'introduction a l'anatomie comparée. 3. Paris, Chez Déterville.

Lozano, R.P.; Pérez-de la Fuente, R.; Barrón, E.; Rodrigo, A.; Viejo, J.L. and Peñalver, E. 2020. Phloem sap in Cretaceous ambers as abundant double emulsions preserving organic and inorganic residues. *Scientific Reports*, 10: 9751.

Luxmoore, R.A. 1981. Moulting and growth in serolid isopods. *Journal of Experimental Marine Biology and Ecology*, 56: 63–85.

Malzahn, E. 1968. Über einen neuen Isopoden aus dem Hauterive Nordwestdeutschlands. *Geologisches Jahrbuch*, 86: 827–834.

Mao, Y.; Liang, K.; Su, Y.; Li, J.; Rao, X.; Zhang, H.; Xia, F.; Fu, Y.; Cai, C. and Huang, D. 2018. Various amberground marine animals on Burmese amber with discussions on its age. *Palaeoentomology*, 1: 91.

Martin, J.W. and Kuck, H.G. 1990. Case 2721 *Bathynomus* A. Milne Edwards 1879 (Crustacea Isopoda): proposed precedence over *Palaega* Woodward 1870. *Bulletin of Zoological Nomenclature*, 47: 27–29.

Matthews, K.J.; Maloney, K.T.; Zahirovic, S.; Williams, S.E.; Seton, M. and Müller, R.D. 2016. Global plate boundary evolution and kinematics since the late Paleozoic. *Global and Planetary Change*, 146: 226–250.

Menzies, R.J.; Bowman, T.E. and Alverson, F.G. 1955. Studies of the biology of the fish parasite *Livoneca convexa* Richardson (Crustacea, Isopoda, Cymothoidae). *Wasmann Journal of Biology*, 13: 277–295.

Mezzalira, S. and Martins-Neto, R.G. 1992. Novos crustáceos Paleozóicos do Estado de São Paulo, com descrição de novos taxa. *Acta Geologica Leopoldensia*, 36: 49–66.

Minelli, A. and Fusco, G. 2013. Arthropod Post-embryonic Development. p. 91–122. In: A. Minelli, G. Boxshall, and G. Fusco (eds), Arthropod Biology and Evolution. Berlin, Heidelberg, Springer Berlin Heidelberg.

Moore, W. and Brusca, R.C. 2003. A monograph on the isopod genus *Colopisthus* (Crustacea: Isopoda: Cirolanidae) with the description of a new genus. *Journal of Natural History*, 37: 1329–1399.

Müller, R.D.; Seton, M.; Zahirovic, S.; Williams, S.E.; Matthews, K.J.; Wright, N.M.; Shephard, G.E.; Maloney, K.T.; Barnett-Moore, N.; Hosseinpour, M.; Bower, D.J. and Cannon, J. 2016. Ocean Basin Evolution and Global-Scale Plate Reorganization Events Since Pangea Breakup. *Annual Review of Earth and Planetary Sciences*, 44: 107–138.

Nagler, C.; Hyžný, M. and Haug, J.T. 2017. 168 million years old "marine lice" and the evolution of parasitism within isopods. *BMC Evolutionary Biology*, 17: 76.

Néraudeau, D.; Perrichot, V.; Batten, D.J.; Boura, A.; Girard, V.; Jeanneau, L.; Nohra, Y.A.; Polette, F.; Saint Martin, S. and Saint Martin, J.-P. 2017. Upper Cretaceous amber from Vendée, north-western France: age dating and geological, chemical, and palaeontological characteristics. *Cretaceous Research*, 70: 77–95.

Paiva, R.J.C. and Souza-Filho, J.F. 2015. A new species of *Dolicholana* Bruce, 1986 (Isopoda, Cymothoidea, Cirolanidae), the first record of the genus from the Atlantic Ocean. *Zootaxa*, 4039: 276.

Pazinato, P.G.; Soares, M.B. and Adami-Rodrigues, K. 2016. Systematic and palaeoecological significance of the first record of Pygocephalomorpha females bearing oöstegites (Malacostraca, Peracarida) from the lower Permian of southern Brazil. *Palaeontology*, 59: 817–826.

Poinar, G. 2018. A new genus of terrestrial isopods (Crustacea: Oniscidea: Armadillidae) in Myanmar amber. *Historical Biology*, 1–6.

Poinar, G.; Archibald, S.B. and Brown, A.E. 1999. New amber deposit provides evidence of Early Paleogene extinctions, paleoclimates and past distributions. *The Canadian Entomologist*, 131: 171–177.

Poinar, G.O. and Hess, R. 1982. Ultrastructure of 40-million-year-old insect tissue. *Science*, 215: 1241–1242.

Polz, H. 2005. Zwei neue Asselarten (Crustacea: Isopoda: Scutocoxifera) aus den Plattenkalken von Brunn (Oberkimmeridgium, Mittlere Frankenalb). *Archaeopteryx*, 23: 67–81.

Poore, G.C.B. and Bruce, N.L. 2012. Global Diversity of Marine Isopods (Except Asellota and Crustacean Symbionts). *PLoS ONE*, 7: e43529.

Price, G.D.; Williamson, T.; Henderson, R.A. and Gagan, M.K. 2012. Barremian–Cenomanian palaeotemperatures for Australian seas based on new oxygen-isotope data from belemnite rostra. *Palaeogeography, Palaeoclimatology, Palaeoecology*, 358–360: 27–39.

Quinney, A.; Mays, C.; Stilwell, J.D.; Zelenitsky, D.K. and Therrien, F. 2015. The range of bioinclusions and pseudoinclusions

preserved in a new Turonian (~90 Ma) amber occurrence from Southern Australia. *PLoS ONE*, 10: e0121307.

Rathbun, M.J. 1935. Fossil Crustacea of the Atlantic and Gulf Coastal Plain. Geological Society of America Special Papers, Vol. 2, 160p.

Riseman, S.F. and Brusca, R.C. 2002. Taxonomy, phylogeny and biogeography of *Politolana* Bruce, 1981 (Crustacea: Isopoda: Cirolanidae). *Zoological Journal of the Linnean Society*, 134: 57–140.

Ross, A. 1998. *Amber*. Cambridge, Harvard University Press, 76p.

Ross, A.J. 1997. Insects in amber. *Geology Today*, 13: 24–28.

Ross, A.J. 2019. Burmese (Myanmar) amber checklist and bibliography 2018. *Palaeoentomology*, 2: 22.

Schädel, M.; Müller, P. and Haug, J.T. 2020. Two remarkable fossil insect larvae from Burmese amber suggest the presence of a terminal filum in the direct stem lineage of dragonflies and damselflies (Odonata). *Rivista Italiana di Palaeontologia e Stratigrafia*, 126: 13–35.

Schädel, M.; Pazinato, P.G.; van der Wal, S. and Haug, J.T. 2019a. A fossil tanaidacean crustacean from the Middle Jurassic of southern Germany. *Palaeodiversity*, 12: 13–30.

Schädel, M.; Perrichot, V. and Haug, J. 2019b. Exceptionally preserved cryptoniscium larvae – morphological details of rare isopod crustaceans from French Cretaceous Vendean amber. *Palaeontologia Electronica*, 22.3.71: 1–46.

Schlüter, T. 1978. Zur systematik und palökologie harzkonservierter Arthropoda einer taphozönose aus dem Cenomanium von NW-Frankreich. *Berliner Geowissenschaftliche Abhandlungen Reihe A: Geologie und Paläontologie*, 9: 1–150.

Schmalfuss, H. 2003. World catalog of terrestrial isopods (Isopoda: Oniscidea). *Stuttgarter Beiträge zur Naturkunde, Serie A*, 654: 1–296.

Schmidt, A.R. and Dilcher, D.L. 2007. Aquatic organisms as amber inclusions and examples from a modern swamp forest. *Proceedings of the National Academy of Sciences*, 104: 16581–16585.

Schmidt, A.R.; Grabow, D.; Beimforde, C.; Perrichot, V.; Rikkinen, J.; Saint Martin, S.; Thiel, V. and Seyfullah, L.J. 2018. Marine microorganisms as amber inclusions: insights from coastal forests of New Caledonia. *Fossil Record*, 21: 213–221.

Schotte, M. 1994. *Annina mannai*, a new isopod from the Ganges river, west Bengal (Crustacea: Isopoda: Cirolanidae). *Proceedings of the Biological Society of Washington*, 107: 268–273.

Scotese, C.R. 2016. PALEOMAP PaleoAtlas for GPlates and the PaleoData Plotter Program, PALEOMAP Project, http://www.earthbyte.org/paleomap-paleoatlas-for-gplates/. Accessed on 11 June 2020.

Scotese, C.R. and Wright, N.M. 2018. PALEOMAP Paleodigital Elevation Models (PaleoDEMS) for the Phanerozoic PALEOMAP Project. Retrieved from https://www.earthbyte.org/paleodem-resource-scotese-and-wright-2018/. Accessed on 11 June 2020.

Serrano-Sánchez, M. de L.; Guerao, G.; Centeno García, E. and Vega, F.J. 2016. Crabs (Brachyura: Grapsoidea: Sesarmidae) as inclusions in Lower Miocene amber from Chiapas, Mexico. *Boletín de la Sociedad Geológica Mexicana*, 68: 37–43.

Serrano-Sánchez, M. de L.; Hegna, T.A.; Schaaf, P.; Pérez, L.; Centeno-García, E. and Vega, F.J. 2015. The aquatic and semiaquatic biota in Miocene amber from the Campo La Granja mine (Chiapas, Mexico): paleoenvironmental implications. *Journal of South American Earth Sciences*, 62: 243–256.

Serrano-Sánchez, M. de L.; Nagler, C.; Haug, C.; Haug, J.T.; Centeno-García, E. and Vega, F.J. 2016. The first fossil record of larval stages of parasitic isopods: cryptoniscus larvae preserved in Miocene amber. *Neues Jahrbuch für Geologie und Paläontologie-Abhandlungen*, 279: 97–106.

Seton, M.; Müller, R.D.; Zahirovic, S.; Gaina, C.; Torsvik, T.; Shephard, G.; Talsma, A.; Gurnis, M.; Turner, M.; Maus, S. and Chandler, M. 2012. Global continental and ocean basin reconstructions since 200Ma. *Earth-Science Reviews*, 113(3–4): 212–270.

Shi, G.; Grimaldi, D.A.; Harlow, G.E.; Wang, J.; Wang, J.; Yang, M.; Lei, W.; Li, Q. and Li, X. 2012. Age constraint on Burmese amber based on U–Pb dating of zircons. *Cretaceous Research*, 37: 155–163.

Sidabalok, C.M. and Bruce, N.L. 2018. Two new species and a new record of *Metacirolana* Kussakin, 1979 (Crustacea: Isopoda: Cirolanidae) from Indonesia. *Zootaxa*, 4370: 519–534.

Sinclair, B.J. 2017. Atelestidae. p. 1257–1260. In: A.H. Kirk-Spriggs and B.J. Sinclair (eds), Manual of Afrotropical Diptera. Volume 2. Nematocerous Diptera and lower Brachycera. Suricata, 5. Pretoria, South African National Biodiversity Institute.

Sinclair, B.J. and Kirk-Spriggs, A.H. 2010. *Alavesia* Waters and Arillo–a Cretaceous-era genus discovered extant on the Brandberg Massif, Namibia (Diptera: Atelestidae). *Systematic Entomology*, 35: 268–276.

Smith, R.D.A. and Ross, A.J. 2018. Amberground pholadid bivalve borings and inclusions in Burmese amber: implications for proximity of resin-producing forests to brackish waters, and the age of the amber. *Earth and Environmental Science Transactions of the Royal Society of Edinburgh*, 107: 239–247.

Soong, K. and Mok, H.-K. 1994. Size and maturity stage observations of the deep-sea isopod *Bathynomus doederleini* Ortmann, 1894 (Flabellifera: Cirolanidae), in Eastern Taiwan. *Journal of Crustacean Biology*, 14: 72–79.

Spassky, N.Y. and Kravtsov, A.G. 1976. The first find of an isopod in the Cenomanian of the Crimea. *Paleontologicheskii Zhurnal*, 10: 151–152.

Stebner, F.; Kraemer, M.M.S.; Ibáñez-Bernal, S. and Wagner, R. 2015. Moth flies and sand flies (Diptera: Psychodidae) in Cretaceous Burmese amber. *PeerJ*, 3: e1254.

Stolley, E. 1910. Über zwei neue Isopoden aus norddeutschem Mesozoikum. *Jahresbericht der Naturhistorischen Gesellschaft zu Hannover*, 60: 191–216.

Strong, K.W. and Daborn, G.R. 1979. Growth and energy utilisation of the intertidal isopod Idotea baltica (Pallas) (Crustacea: Isopoda). *Journal of Experimental Marine Biology and Ecology*, 41: 101–123.

Tabacaru, I. and Danielopol, D.L. 1996. Phylogénie des Isopodes terrestres. *Comptes rendus de l'Académie des sciences. Série 3, Sciences de la vie*, 319: 71–80.

Tait, J. 1918. V.—Experiments and Observations on Crustacea: Part II. Moulting of Isopods. *Proceedings of the Royal Society of Edinburgh*, 37: 59–68.

van der Wal, S. and Haug, J.T. 2020. Shape of attachment structures in parasitic isopodan crustaceans: the influence of attachment site and ontogeny. *PeerJ*, 8: e9181.

Vega, F.J.; Bruce, N.L.; González-León, O.; Jeremiah, J.; Serrano-Sánchez, M. de L.; Alvarado-Ortega, J. and Moreno-Bedmar, J.A. 2019. Lower Cretaceous marine isopods (Isopoda: Cirolanidae, Sphaeromatidae) from the San Juan Raya and Tlayúa formations, Puebla, Mexico. *Journal of Crustacean Biology*, 39: 121–135.

Voigt, S.; Wilmsen, M.; Mortimore, R.N. and Voigt, T. 2003. Cenomanian palaeotemperatures derived from the oxygen isotopic composition of brachiopods and belemnites: evaluation of Cretaceous palaeotemperature proxies. *International Journal of Earth Sciences*, 92: 285–299.

Wägele, J.-W. 1989. Evolution und phylogenetisches System der Isopoda: Stand der Forschung und neue Erkenntnisse. *Zoologica* (Stuttgart), 140: 1–262.

Wägele, J.-W. and Brandt, A. 1988. *Protognathia* n. gen. *bathypelagica* (Schultz, 1977) rediscovered in the Weddell Sea: A missing link between the Gnathiidae and the Cirolanidae (Crustacea, Isopoda). *Polar Biology*, 8: 359–365.

Waggoner, B.M. 1994. An aquatic microfossil assemblage from Cenomanian amber of France. *Lethaia*, 27: 77–84.

Waloszek, D. 1999. On the Cambrian diversity of Crustacea. p. 3–27. In: F.R. Schram and J.C. von Vaupel Klein (eds), Crustaceans and the Biodiversity Crisis. Proceedings of the Fourth International Crustacean Congress. Leiden, Brill.

Weitschat, W.; Brandt, A.; Coleman, C.O.; Andersen, N.M.; Myers, A.A. and Wichard, W. 2002. Taphocoenosis of an extraordinary arthropod community in Baltic amber. *Mitteilungen aus dem Geologisch-Paläontologischen Institut der Universität Hamburg*, 86: 189–210.

Wichard, W.; Gröhn, C. and Seredszus, F. 2009. Aquatic Insects in Baltic Amber - Wasserinsekten im Baltischen Bernstein. Remagen, Verlag Kessel, 336p.

Wieder, R.W. and Feldmann, R.M. 1989. *Palaega goedertorum*, a fossil isopod (Crustacea) from late Eocene to early Miocene rocks of Washington State. *Journal of Paleontology*, 63: 73–80.

Wieder, R.W. and Feldmann, R.M. 1992. Mesozoic and Cenozoic fossil isopods of North America. *Journal of Paleontology*, 66: 958–972.

Wilson, G.D.F. 2003. A new genus of Tainisopidae fam. nov. (Crustacea: Isopoda) from the Pilbara,Western Australia. *Zootaxa*, 245: 1–20.

Wilson, G.D.F.; Paterson, J.R. and Kear, B.P. 2011. Fossil isopods associated with a fish skeleton from the Lower Cretaceous of Queensland, Australia - direct evidence of a scavenging lifestyle in Mesozoic Cymothoida: Scavenging isopod crustaceans from the Lower Cretaceous. *Palaeontology*, 54: 1053–1068.

Woodward, H. 1870. I.—Contributions to British Fossil Crustacea. *Geological Magazine*, 7: 493.

Xing, L.; Sames, B.; McKellar, R.C.; Xi, D.; Bai, M. and Wan, X. 2018. A gigantic marine ostracod (Crustacea: Myodocopa) trapped in mid-Cretaceous Burmese amber. *Scientific Reports*, 8: 1365.

Yu, T.; Kelly, R.; Mu, L.; Ross, A.; Kennedy, J.; Broly, P.; Xia, F.; Zhang, H.; Wang, B. and Dilcher, D. 2019. An ammonite trapped in Burmese amber. *Proceedings of the National Academy of Sciences*, 116: 11345-11350.

Yu, T.-T.; Wang, B. and Jarzembowski, E. 2018. First record of marine gastropods (wentletraps) from mid-Cretaceous Burmese amber. *Palaeoworld*, 28: 508–513.

Zhang, W.W. 2017. Frozen dimensions. The fossil insects and other invertebrates in amber. Chongqing, Chongqing University Press, 692p.

Zhao, X.; Zhao, X.; Jarzembowski, E.A. and Wang, B. 2019. The first whirligig beetle larva from mid-Cretaceous Burmese amber (Coleoptera: Adephaga: Gyrinidae). *Cretaceous Research*, 99: 41–45.

Zheng, D.; Chang, S.-C.; Perrichot, V.; Dutta, S.; Rudra, A.; Mu, L.; Kelly, R.S.; Li, S.; Zhang, Q.; Zhang, Q.; Wong, J.; Wang, J.; Wang, H.; Fang, Y.; Zhang, H. and Wang, B. 2018. A Late Cretaceous amber biota from central Myanmar. *Nature Communications*, 9: 1–6.